

1 **An analysis of the variability of  $\delta^{13}\text{C}$  in macroalgae from the Gulf of California**

2

3 Roberto Velázquez-Ochoa<sup>a</sup>, María Julia Ochoa-Izaguirre<sup>b</sup>, Martín F. Soto-Jiménez<sup>c\*</sup>

4 <sup>a</sup>Posgrado en Ciencias del Mar y Limnología, Universidad Nacional Autónoma de México, Unidad  
5 Académica Mazatlán, Mazatlán, Sinaloa 82040, México

6 <sup>b</sup>Facultad de Ciencias del Mar, Universidad Autónoma de Sinaloa. Paseo Claussen s/n, Mazatlán,  
7 Sinaloa 82000, México

8 <sup>c</sup>Unidad Académica Mazatlán, Instituto de Ciencias del Mar y Limnología, Universidad Nacional  
9 Autónoma de México (UAM-ICMyL-UNAM), Mazatlán Sinaloa, 82040, México.

10

11 Correspondent author:

12 Telephone number: +52 (669) 9852845 to 48.

13 Fax number: +52 (669) 9826133

14 E-mail: [martin@ola.icmyl.unam.mx](mailto:martin@ola.icmyl.unam.mx)

15

16

17 **Abstract**

18 The isotopic composition of carbon in macroalgae ( $\delta^{13}\text{C}$ ) is highly variable, and its prediction is very  
19 complex concerning terrestrial plants. To contribute to the knowledge about the variations and  
20 determinants of  $\delta^{13}\text{C}$ -macroalgal, we analyzed a large stock of specimens that vary in taxa and  
21 morphology and that inhabit shallow marine habitats in the Gulf of California (GC) featured by  
22 distinctive environmental conditions. A large  $\delta^{13}\text{C}$  variability (-34.6‰ to -2.2‰) was observed,  
23 mainly explained by the life form (taxonomy, morphology, and structural organization), and  
24 modulated by the interaction between habitat features and environmental conditions. The intertidal  
25 zone specimens had fewer negative  $\delta^{13}\text{C}$  values than in the subtidal zone. Except for pH,  
26 environmental conditions of the seawater do not contribute to the  $\delta^{13}\text{C}$  variability. Specimens of the  
27 same taxa showed  $\delta^{13}\text{C}$  similar patterns, to increase or decrease, with latitude (21°-30°N).  $\delta^{13}\text{C}$ -  
28 macroalgal provides information on the inorganic carbon source used for photosynthesis ( $\text{CO}_2$   
29 diffusive entry vs  $\text{HCO}_3^-$  active uptake). Most species showed a  $\delta^{13}\text{C}$  belong into a range that  
30 indicates a mix of  $\text{CO}_2$  and  $\text{HCO}_3^-$  uptake (strategy 2:  $-10 < \delta^{13}\text{C} > -30\text{‰}$ ); however, the  $\text{HCO}_3^-$  uptake  
31 by active transport (strategy 1:  $\delta^{13}\text{C} > -10\text{‰}$ ) is also widespread among GC macroalgae. Ochrophyta  
32 presented a high number of species with  $\delta^{13}\text{C} > -10\text{‰}$ . Few species belonging to Rhodophyta relied  
33 on  $\text{CO}_2$  diffusive entry (strategy 3:  $\delta^{13}\text{C} < -30\text{‰}$ ) exclusively. Few calcifying macroalgae species  
34 using  $\text{HCO}_3^-$  and diffusive  $\text{CO}_2$  (strategy 4) were also collected, such as *Amphiroa* and *Jania*. The  
35  $\delta^{13}\text{C}$  values of macroalgae integrate the isotope discrimination during carbon assimilation and, to a  
36 lesser extent, during the respiration across its lifecycle, thus providing useful information on the  
37 physiological and environmental status of macroalgae.

38 **Keywords:**  $\delta^{13}\text{C}$ -macroalgal, carbon-concentrating mechanisms,  $\text{CO}_2$  diffusive proxy

39

## 40        **1. Introduction**

41    Macroalgae show a wide diversity of thallus morphologies (e.g., filamentous, articulated, flattened),  
42    structural organization (e.g., surface area/volume ratio), and various photosynthetic pigments (e.g.,  
43    Chlorophyll *a*, *b*, phycocyanin) (Lobban and Harrison, 1994). Based on these features, macroalgae  
44    can be classified into only three Phyla, according to the predominant pigment contents in the thallus,  
45    or into dozens of groups considering the interaction of morphologies and photosynthetic pigments  
46    (Littler and Littler, 1980; Littler & Arnold, 1982; Balata et al., 2011). For example, the mixture of  
47    chlorophyll (*a*, *b*) and carotenoids is dominant in Chlorophyta; chlorophyll (*a*, *c*) and fucoxanthin  
48    carotenoid is dominant in Ocrophyta, while Rhodophyta contains chlorophyll (*a*, *d*), carotenoid, and  
49    a mixture of phycobilin (e.g., phycocyanin, phycoerythrina, allophycocyanin) (Bold and Wynne,  
50    1978; Masojidek et al., 2004; Gateau et al., 2017). Both traits work as an excellent approximation to  
51    explain the fundamentals of metabolism, growth, zonation, and colonization (Littler and Littler,  
52    1980; Littler and Arnold, 1982; Nielsen and Sand-Jensen, 1990; Vásquez-Elizondo and Enríquez,  
53    2017).

54    The thickness of the thallus as a propriety of morphology influences the diffusion boundary layer on  
55    surface of the macroalgal, where they carry out the absorption of essential ions and dissolved gases  
56    (Hurd, 2000; San-Ford and Crawford, 2000). In marine environments, where  $\text{pH} \sim 8.1 \pm 1$ ,  $\text{HCO}_3^-$   
57    accounts for 98% of the total DIC due to the low diffusion rate of  $\text{CO}_2$  in seawater that results in a  
58    high  $\text{HCO}_3^-:\text{CO}_2$  ratio (150:1) (Sand-Jensen and Gordon, 1984). The limitations to growth imposed  
59    by low  $\text{CO}_2$  concentrations in seawater are compensated by carbon concentration mechanisms  
60    (CCMs) in most macroalgae that increase the internal inorganic carbon concentration near the site  
61    of RuBisCo activity (Giordano et al., 2005). Therefore, the absorption of  $\text{HCO}_3^-$  by most macroalgae  
62    is the main source of inorganic carbon for photosynthesis, but some species depend exclusively on  
63    the use of dissolved  $\text{CO}_2$  that enters cells by diffusion (Maberly et al., 1992; Beardall and Giordano,

64 2002; Raven et al., 2002a, b; Giordano et al., 2005). Hence, macroalgal species with productivity  
65 limited by lacking CCM's (have low plasticity for carbon inorganic forms uptake) seems to be  
66 restricted to subtidal habitats and composed mainly by red macroalgae (but without a morphological  
67 patron apparent) (Cornwall et al., 2015, Kübler and Dungeon, 2015). The rest of the macroalgae with  
68 CCM occupies from the intertidal to the deep subtidal.

69 Nevertheless, marine ecosystems have many environmental factors, including habitat features and  
70 environmental conditions in seawater that modify the main macroalgae photosynthesis drivers as  
71 light (Anthony et al., 2004; Johansson and Snoeijs, 2014), DIC (Zeebe and Wolf-Gladrow, 2001;  
72 Brodeur et al., 2019), and inorganic nutrients (Teichberg et al., 2010; Ochoa-Izaguirre and Soto-  
73 Jiménez, 2015). These factors could generate negative consequences for their productivity,  
74 principally when they cause resources limitation. Each factor varies from habitat to habitat (e.g.,  
75 local scale: from intertidal to subtidal and global scale: from temperate to tropical regions), and as  
76 in response to these environmental changes, macroalgae can modulate their photosynthetic  
77 mechanism (Lapointe and Duke, 1984; Dudgeon et al., 1990; Kübler and Davison 1993, Young et  
78 al., 2005). The modulation, to increase their photosynthetic activity (up-and-down-regulation  
79 processes), implies a physiological acclimation enhancing the transport of DIC ( $\text{CO}_2$ ,  $\text{HCO}_3^-$ ) into  
80 the cell and its fixation rates (Madsen and Maberly, 2003; Klenell et al., 2004; Zou et al., 2004;  
81 Giordano et al., 2005; Enríquez and Rodríguez-Román, 2006; Rautemberger et al., 2015).

82 The  $\delta^{13}\text{C}$  on the thallus of marine macrophytes is a proxy used to identify  $\text{CO}_2$  or  $\text{HCO}_3^-$  source in  
83 photosynthesis and to infer the presence or absence of CCM's (Maberly et al., 1992; Raven et al.,  
84 2002a). Also, the  $\delta^{13}\text{C}$  signal in the algal thallus can be used as an indicator of the physiological state  
85 of photosynthetic metabolism (Kim et al., 2014; Kübler and Dungeon, 2015). For example,  $\delta^{13}\text{C}$   
86 variability depends, in part, on the life forms as taxonomy, morphology, and structural organization  
87 (Mercado et al., 2009, Marconi et al., 2011, Lovelock et al., 2020), but also is modulated by the

88 interaction to environmental conditions (e.g., light, DIC, and nutrients) (Cornelisen et al., 2007;  
89 Dudley et al., 2010; Carvalho et al., 2010ab; Mackey et al., 2015; Rautenberger et al., 2015).  
90 In this study, our objective was to investigate the contributions of life form, the changes in the habitat  
91 features, and environmental conditions to the  $\delta^{13}\text{C}$  macroalgal variability in communities in the Gulf  
92 of California (GC). To reach our objective, we collected a large stock of macroalgae specimens of a  
93 diversity of species characterized by a variety of morphological and physiological properties.  
94 Besides high diversity, in terms of life forms, we selected various shallow marine habitats along a  
95 latitudinal gradient in the GC or the sample collection, characterized by unique and changing  
96 environmental factors. The GC features abundant and diverse macroalgae populations, which are  
97 acclimated and adapted to diverse habitats with environmental conditions, determining the light,  
98 DIC, and nutrients availability. The  $\delta^{13}\text{C}$  signal from the thallus of macroalgae was also used to infer  
99 carbon uptake strategies in macroalgae communities in the GC in function of taxa and environmental  
100 factors (Maberly et al., 1992; Raven et al., 2002; Hepburn et al., 2011; Díaz-Pulido et al., 2016).  
101 Because the GC is a subtropical zone with high irradiance and specimens were collected in the  
102 intertidal and subtidal zone, we expect to find a high proportion of species with active uptake  $\text{HCO}_3^-$   
103 ( $\delta^{13}\text{C} > -10\text{‰}$ ). A third objective was to explore any geographical pattern in the  $\delta^{13}\text{C}$  macroalgal along  
104 and between the GC bioregions. Previous studies have indicated changes in the  $\delta^{13}\text{C}$  signal with  
105 latitude, mainly related to the light and temperature (Mercado et al., 2009; Marconi et al., 2011;  
106 Stepien, 2015; Hofmann and Heesch, 2018; Lovelock et al., 2020). Macroalgae as biomonitor  
107 constitute an efficient tool in monitoring programs in large geographical regions (Balata et al., 2011)  
108 and for environmental impact assessments (Ochoa-Izaguirre and Soto-Jiménez, 2015).

## 109 **2. Materials and Methods**

### 110 **2.1. Gulf of California description**

111 The Gulf of California is a subtropical, semi-enclosed sea of the Pacific coast of Mexico, with  
112 exceptionally high productivity being the most important fishing regions for Mexico and one of the  
113 most biologically diverse worldwide marine areas (Zeitzschel, 1969; Espinosa-Carreón and Valdez-  
114 Holguín 2007; Lluch-Cota et al., 2007; Páez-Osuna et al., 2017). GC represents only 0.008% of the  
115 area covered by the seas of the planet (265,894 km<sup>2</sup>, 150 km wide, and 1000 km long covering >9  
116 degrees latitude) but has a high physiographic diversity and is biologically mega-diverse with many  
117 endemic species, including ~ 766 macrofauna species and/or sub-species where the major number  
118 belong to Arthropoda (118 spp) and Mollusca (460) taxas (Brusca et al., 2005; Wilkinson et al.,  
119 2009; Espinosa-Carreón and Escobedo-Urías, 2017) and 116 macroalgae species (Norris, 1975,  
120 1985; Espinoza-Avalos, 1993).

121 Regionalization criteria of the GC include phytoplankton distribution (Gilbert and Allen, 1943),  
122 topography (Rusnak et al., 1964) and depth (Álvarez-Borrego, 1983), oceanographic characteristics  
123 (Roden and Emilson, 1979; Álvarez-Borrego, 1983; Marinone and Lavin 2003), biogeography  
124 (Santamaría-del-Ángel et al., 1994), and bio-optical characteristics (Bastidas-Salamanca et al.,  
125 2014). The topography is variable along with GC, includes submarine canyons, basins, and variable  
126 continental platforms. Besides, GC presents complex hydrodynamic processes, including internal  
127 waves, fronts, upwelling, vortices, mixing of tides. The gulf's coastline is divided into three shores:  
128 extensive rocky shores, long sandy beaches, numerous scattered estuaries, coastal lagoons, and open  
129 muddy bays tidal flats, and coastal wetlands (Lluch-Cota et al., 2007).

130 The Gulf of California is different in the north and the south, related to a wide range of  
131 physicochemical factors. The surface currents seasonally change direction and flow to the southeast  
132 with maximum intensity during the winter and to the northwest in summer (Roden (1958). The  
133 northern part is very shallow (<200 m deep averaged), divided into Upper Gulf, northern Gulf, and

134 Grandes Islas. The surrounding deserts largely influence this region (Norris, 2010) shows marked  
135 seasonal changes in coastal seawater temperatures (Martínez-Díaz de León et al., 2006; Marinone,  
136 2007). Tidal currents induce a significant cyclonic circulation through June to September and  
137 anticyclonic from November to April (Carrillo et al., 2002; Bray, 1988a; Velasco-Fuentes and  
138 Marinone, 1999; Martínez-Díaz-de-León, 2001). The southern part consists of a series of basins  
139 whose depths increase southwards (Fig. 1). The intertidal macroalgae in the southern region are  
140 subject to desiccation, mostly during summer. The water column's physicochemical characteristics  
141 are highly influenced by the contrasting climatic seasons in the GC, the dry season (nominally from  
142 November to May), and the rainy season (from June to October). Annual precipitation ( $1,080 \text{ mm y}^{-1}$   
143  $^1$ ) and evaporation ( $56 \text{ mm y}^{-1}$ ) rates registered during the past 40 years were  $881 \pm 365 \text{ mm y}^{-1}$  and  
144  $53 \pm 7 \text{ mm y}^{-1}$ , respectively (CNA, 2012).

145 Previous macroalgae floristic studies of the GC, report around 669 species, including 116 endemic  
146 species (Norris, 1975; Espinoza-Avalos, 1993; Pedroche and Senties, 2003). Many endemic  
147 species currently have a wide distribution along the Pacific Ocean coast, but with GC origin  
148 (Dreckman, 2002; Aguilar-Rosas et al., 2014). Based on oceanographic characteristics (Roden and  
149 Groves, 1959) and in the endemic species distribution (Aguilar Rosas and Aguilar Rosas, 1993;  
150 Espinoza-Avalos, 1993), the GC can be classified into three phycofloristic zones: 1) the first zone  
151 located from the imaginary line connecting San Francisquito Bay, B.C. to Guaymas, Sonora, with  
152 51 endemic species. 2) the second zone with an imaginary line from La Paz bay (B.C.S.) to  
153 Topolobampo (Sinaloa) with 41 endemic species. 3) the third zone is located with an imaginary line  
154 from Cabo San Lucas (B.C.S.) to Cabo Corrientes (Jalisco) with 10 endemic species. Besides, 14  
155 endemic species are distributed throughout the GC (Espinoza-Ávalos, 1993). The macroalgal  
156 communities are subject to the changing environmental conditions in the diverse habitats in the GC

157 that delimits their zonation, which tolerates a series of anatomical and physiological adaptations to  
158 water movement, temperature, sun exposure, and light intensities, low pCO<sub>2</sub>, desiccation (Espinoza-  
159 Avalos 1993).

## 160 **2.1 Macroalgae sampling**

161 In this study, the GC coastline (21°-30°N latitude) was divided into six coastal sectors based on the  
162 three phycofloristic zones along peninsular and continental GC coastlines (Fig. 1a). In each coastal  
163 sector, selected ecosystems and representative habitats were sampled based on macroalgae  
164 communities' presence and habitat characterization. Habitats were classified by substrate type (e.g.,  
165 sandy-rock, rocky shore), hydrodynamic (slow to faster water flows), protection level (exposed or  
166 protected sites), and immersion level (intertidal or subtidal) (Fig. 1b).

167 Based on the local environmental factors, macroalgae specimens (4-5) of the most representative  
168 species were gathered by hand (free diving) during low tide. A total of 809 composite samples were  
169 collected from marine habitats along both GC coastlines. The percentages of specimens collected for  
170 the substrate type were sandy-rock 28% and rocky shores 72% based on the habitat features. Related  
171 to the hydrodynamic, 30% of the specimens were collected in habitats with slow to moderate and  
172 70% with moderate to fast water movement. Regarding the protection level, 57% were exposed  
173 specimens, and 43% were protected. Finally, 56% were intertidal and 44% subtidal macroalgae  
174 organisms concerning the emersion level. About half of the protected specimens were collected in  
175 isolated rock pools, which was noted.

176 In 4-5 sites of each habitat, we measured *in situ* the salinity, temperature, and pH by using a  
177 calibrated multiparameter sonde (Y.S.I. 6600V) and the habitat characteristics mentioned above  
178 noted. Besides, composite water samples were collected for complementary analysis of nutrient,



179 alkalinity (and their chemical components), and  $\delta^{13}\text{C}$ -DIC (data non-included). Briefly, the  
180 representative habitats were classified by pH levels in  $>9.0$  “alkalinized”,  $7.9$ - $8.2$  ‘typical’ and  $<7.9$   
181 “acidified”. Based on the temperature in colder  $<20^\circ\text{C}$ , typical  $20$ - $25^\circ\text{C}$ , and warmer  $>25^\circ\text{C}$ . 72% of  
182 the specimens were collected at typical pH values, 22% in alkalinized and 6% in acidified seawater.  
183 Regarding the temperature, about 55% of the specimens were collected at typical, 31% at warmer,  
184 and 14% at colder seawaters. Regarding salinity, most of the ecosystems showed typical values for  
185 seawater ( $35.4 \pm 0.91$  ups, from 34.5 to 36.1 ups). In this study, the collection surveys were conducted  
186 during spring (March-April) and dry season (nominally from November to May) from 2009 to 2014.  
187 Only in few selected ecosystems located at C1 and C2 sectors, one sampling survey was conducted  
188 at the end of the rainy season (nominally from June to October in 2014). Thus, these ecosystems  
189 were possible to include habitat with a salinity range varying from estuarine ( $23.5 \pm 3.0$  ups) to  
190 hypersaline ( $42.7 \pm 7.0$  ups) values. These habitats were mainly isolated rockpools, and only a few  
191 were sites near tidal channels receiving freshwater discharges. About 95% of the specimens were  
192 collected at typical seawater salinity (34-36 ups) and only 1.5 and 3.5% in estuarine ( $<30$  ups) and  
193 hypersaline ( $>37$  ups) environments, respectively. Detailed information on the selected shallow  
194 marine ecosystems, habitat characterization, and environmental conditions is summarized in the  
195 inserted table in Fig. 1.

## 196 **2.2 Macroalgae processing and analysis of the isotopic composition of carbon**

197 The collected material was washed *in situ* with surface seawater to remove the visible epiphytic  
198 organisms, sediments, sand, and debris and then thoroughly rinsed with MilliQ water. The composite  
199 samples were double-packed in a plastic bag, labeled with the locality's name and collection date,  
200 placed in an ice-cooler box to be kept to  $4^\circ\text{C}$ , and immediately transported to the laboratory UAS-  
201 Facimar in Mazatlán. In the field, sample aliquots were also preserved in 4% v/v formaldehyde

202 solution for taxonomic identification to the genus or species level (when possible). The following  
203 GC macroalgal flora identification manuals were consulted: Dawson, 1944; 1954; 1956; 1961; 1962;  
204 1963; Setchell and Gardner, 1920; 1924; Abbott and Hollenberg, 1976; Ochoa-Izaguirre et al., 2007;  
205 Norris, 2010).

206 In the laboratory, macroalgae samples were immediately frozen at -30°C until analysis. Then,  
207 samples were freeze-dried at -38°C and 40 mm Hg for 3 days, upon which they were ground to a  
208 fine powder and exposed to HCl vapor for 4 h (acid-fuming) to remove carbonates and dried at 60°C  
209 for 6 h (Harris et al. 2001). Aliquots of ~5 mg were encapsulated in tin cups (5x9 mm) and stored in  
210 sample trays until analysis. Macroalgae samples were sent to the Stable Isotope Facility (SIF) at the  
211 University of California at Davis, CA, USA. Natural <sup>13</sup>C relative abundance relative to <sup>12</sup>C in  
212 samples was determined with mass spectrometry, using a Carlo Erba elemental analyzer attached to  
213 a Finnigan Delta S mass spectrometer equipped with a Europa Scientific stable isotope analyzer  
214 (ANCA-NT 20-20) and a liquid/solid preparation unit (PDZ, Europa, Crewz, UK). Isotope ratios of  
215 the samples were calculated using the equation  $\delta (\text{‰}) = (R_{\text{sample}}/R_{\text{standard}} - 1) \times 1000$ , where  $R = {}^{13}\text{C}/{}^{12}\text{C}$ .  
216 The  $R_{\text{standard}}$  is relative to the international V-PDB (Vienna PeeDee Belemnite) standard. During the  
217 isotopic analysis, the SIF lab used different certified reference materials (e.g., IAEA-600, USGS-40,  
218 USGS-41, USGS-42, USGS-43, USGS-61, USGS-64, and USGS-65) for the analytical control  
219 quality. The analytical uncertainties reported for the SIF lab were 0.2‰ for  $\delta^{13}\text{C}$   
220 (<https://stableisotopefacility.ucdavis.edu/13cand15n.html>). We also included triplicate aliquots of  
221 several specimens of the same species and condition, collected from one patch, or attached to the  
222 same substrate, to assess the method error by sampling and processing procedural. The  
223 methodological uncertainties were <0.4‰.

### 224 **2.3. Analysis of $\delta^{13}\text{C}$ -macroalgal variability**

225 The variability of  $\delta^{13}\text{C}$  values in macroalgae was analyzed in function of the taxonomy (phylum,  
226 genus, and species) and morpho-functional groups (e.g., thallus structure, growth form, branching  
227 pattern, and taxonomic affinities; Balata et al. 2011; Ochoa-Izaguirre and Soto-Jiménez, 2015).

228 The carbon fixation strategies in the macroalgae communities of the GC were identify by  $\delta^{13}\text{C}$   
229 (Hepburn et al., 2011; Díaz-Pulido et al., 2016), in agreement with the Maberly et al. (1992) and  
230 Raven et al. (2002) thresholds. So, macroalgae were classified into four strategies for DIC uptake:  
231 1) CCM-only by active uptake  $\text{HCO}_3^-$  ( $\delta^{13}\text{C} > -10\%$ ), 2) CCM active uptake  $\text{HCO}_3^-$  and/or diffusive  
232 uptake  $\text{CO}_2$  ( $\delta^{13}\text{C} < -11$  to  $-30\%$ ), 3) Non-CCM,  $\text{CO}_2$  by diffusion only ( $\delta^{13}\text{C} < -30\%$ ), 4) Calcifying  
233 with different carbon-use strategies related to different modes of calcification. The measured  $\delta^{13}\text{C}$ -  
234 macroalgal signals are integrative of the discrimination by photosynthesis ( $\Delta^{13}\text{C}_p$ ) on the carbon  
235 source ( $\delta^{13}\text{C}$ -DIC in seawater), respiration ( $\Delta^{13}\text{C}_r$ ), and probable  $\text{CO}_2$  leak out inside the cell  
236 during the CCM process (Sharkey and Berry, 1985; Raven et al., 2005; Carvalho et al., 2009a,b).

237 To find a geographic pattern associated with the  $\delta^{13}\text{C}$  signal of macroalgae in this study, macroalgae  
238 were grouped according to their characteristics morpho-functional proposed initially by Littler and  
239 Littler (1980) and modified by Balata et al. (2011). Not all morphofunctional groups and taxon were  
240 present in every site during each sampling survey, and the sample size in each group varied for taxa,  
241 location, and time.

242 A basic statistical analysis of  $\delta^{13}\text{C}$  values in different macroalgae groups was applied to distribute  
243 and calculate the arithmetic mean, standard deviation, minimum and maximum. Because not all  
244 macroalgal species were present in sufficient numbers at different collection habitats, several  
245 macroalgal groups were not considered for statistical analysis. Regarding the life form, we compared  
246 among morphofunctional groups, taxon collected in the same habitat (within-subjects factor) by  
247 multivariate analysis of variance. When differences were noted, a Tukey-Kramer HSD (Honestly

248 Significant Difference) test was performed. Besides, variations of  $\delta^{13}\text{C}$  macroalgal in specimens of  
249 the same morpho-functional and taxon collected in different habitats were also investigated with a  
250 Kruskal-Wallis test.

251 In this study, the relationships between  $\delta^{13}\text{C}$  with each independent variable related to the inherent  
252 macroalgae properties (morphology and taxon), biogeographical collection zone (GC coastline and  
253 coastal sector), habitat features (substrate, hydrodynamic, protection, and emersion level) and  
254 environmental conditions (temperature, pH, and salinity) were examined through simple and  
255 multiple linear regression analyses. Excepting temperature, pH, and salinity, most of the independent  
256 variables are categorical independent variables. However, these continue variables were also  
257 categorized, such as previously was described. Analyses of simple linear regression were performed  
258 to establish the relationships between  $\delta^{13}\text{C}$ -macroalgal with each environmental parameter analyzed  
259 as possible driving factors (e.g., temperature, salinity, pH). Multiple linear regression analyses were  
260 conducted to evaluate the combined effects of those independent variables (macroalgae properties,  
261 biogeographical collection zone, habitat features, and environmental conditions) on the  $\delta^{13}\text{C}$ -  
262 macroalgal. In the multivariable regression model, the dependent variable,  $\delta^{13}\text{C}$ -macroalgal, is  
263 described as a linear function of the independent variables  $X_i$ , as follows:  $\delta^{13}\text{C}$ -macroalgal = a +  
264  $b_1(X_1) + b_2(X_2) + \dots + b_n(X_n)$  (1). Where a is regression constant (it is the value of intercept and its  
265 value is zero);  $b_1$ ,  $b_2$ , and  $b_n$ , are regression coefficients for each independent variable  $X_i$ . From each  
266 one of the fitted regression models, we extracted the estimated regression coefficients for each of the  
267 predictor variables (e.g., Bayesian Information Criterion (BIC), Akaike Information Criterion (AIC),  
268 root-mean-square error (RMSE), Mallow's Cp criterion, F Ratio test, p-value for the test (Prob > F),  
269 coefficients of determination ( $R^2$ ) and the adjusted  $R^2$  statistics) (SAS Institute Inc., 2018). All  
270 regression coefficients were used as indicators of the quality of the regression (Draper and Smith,

1998; Burnham and Anderson, 2002). Kolmogorov-Smirnov normality test was applied for all variables, and all were normally distributed. Most of the  $\delta^{13}\text{C}$  values in each group showed a normal distribution. For all statistical tests, a probability  $P < 0.05$  was used to determine statistical significance. The statistical analysis of the results was done using JMP 14.0 software (SAS Institute Inc.).

### 3. Results

#### 3.1. Taxonomy and morpho-functional groups

Sampled specimens belong to three Phyla, 63 genera, and 167 species. The Phyla were identified as Chlorophyta (25%), Ochrophyta (22%), and Rhodophyta (53%). The most representative genus (and their species) were *Ulva* (*U. lactuca*, *U. lobata*, *U. flexuosa*, and *U. intestinalis*), *Codium* (*C. amplivesiculatum* and *C. simulans*), *Chaetomorpha* (*C. antenina*), *Padina* (*P. durvillaei*), *Dictyota* (*D. dichotoma*), *Colpomenia* (*C. tuberculata* and *C. sinuosa*), *Sargassum* (*S. sinicola* and *S. horridum*), *Amphiroa* (*Amphiroa* spp.), *Spyridia* spp, *Polysiphonia* spp., *Gymnogongrus* spp., *Gracilaria* (*G. vermiculophylla*, *G. pacifica* and *G. crispate*), *Hypnea* (*H. pannosa* and *H. johnstonii*) *Grateloupia* (*G. filicina* and *G. versicolor*), and *Laurencia* (*L. papillosa* and *L. pacifica*). An analysis of the biogeographical diversity among sectors evidenced that P3 (43 genera of 63, 68%) and C3 (63%) at north recorded the highest number of the genus, followed by C1 (38%) and P1 (29%) at the south, and P2 (27%) and C2 (22%). The same pattern was observed in the species richness, zones P3 (94 of 167 species, 56%) and C3 (52%) at the north, C1 (34%) and P1 (25%) at the south, and C2 and P2 (19-20%) at the center. In our study, the endemic species includes Chlorophyta *Codium amplivesiculatum*, Rhodophyta *Laurencia papillosa*, *Chondracanthus squarrulosa*, *Gracilaria spinigera*, and *Gracilaria subsecundata*, and Ochrophyta *Cutleria hancockii*, *Sargassum*

293 *herphorizum*, *Sargassum johnstonii*.

294 The morphofunctional groups identified were 21, of which the most common were C-tubular (6 spp.,  
295 n=69; C-Blade-like (6 spp, n=55); C-Filamentous uniseriate (17 spp, n=49); C-Erect thallus (5 spp,  
296 n=33); O-Compressed with branched or divided thallus (19 spp., n=92); O-Thick leathery  
297 macrophytes (12 spp., n=104); O-Hollow with spherical or subspherical shape (4spp, n=87); R-  
298 Large-sized corticated (57 spp., n=225); R-Filamentous uniseriate and pluriseriate with erect thallus  
299 (9 spp., n=48); and R-Large-sized articulated corallines (6 spp, n=17). The diversity, in terms of  
300 presence/absence of the morphofunctional groups, varied among coastline sectors, higher in C3 (16  
301 of 21, 76%) and P3 (71%) at the north, followed by C1 (57%) and P1 (48%) at the south, and C2  
302 and P2 and (42-48%) at the center of both GC coastlines. Detailed information on macroalgae  
303 specimens collected (ecosystem, habitat, number of composite samples, morphological group, and  
304 taxon) is given as Supplementary Information (Table SI-1).

### 305 **3.2. $\delta^{13}\text{C}$ -macroalgal variability in function of taxonomy and morpho-functional groups**

306 The variability of  $\delta^{13}\text{C}$  values in macroalgae was analyzed by taxon in the phylum, genus, species,  
307 and morphofunctional groups.  $\delta^{13}\text{C}$  values analyzed by phylum showed a unimodal distribution with  
308 a peak at  $-14 \pm 1.4\text{‰}$  (Fig 2 and 3), where Ochrophyta displayed the values from  $-21.5$  to  $-2.2\text{‰}$  ( $-$   
309  $12.5 \pm 3.7\text{‰}$ ), significantly higher to Chlorophyta ( $-25.9$  to  $-5.5\text{‰}$ ,  $-14.5 \pm 3.0\text{‰}$ ) and Rhodophyta that  
310 showed the largest range ( $-34.6$  to  $-4.5\text{‰}$ ,  $-14.8 \pm 3.9\text{‰}$ ). The  $\delta^{13}\text{C}$ -macroalgal values (average $\pm$ SD)  
311 for the genus of Chlorophyta, Ochrophyta, and Rhodophyta (Fig. 3.) varied from  $-33.8 \pm 1.1\text{‰}$  for  
312 *Schizymenia* to  $-7.8 \pm 0.7\text{‰}$  for *Amphiroa*. Based on the highest values, specimens of three Phyla with  
313 relatively high  $\delta^{13}\text{C}$  values ( $> -10\text{‰}$ ), evidenced the presence of CCM's by active uptake of  $\text{HCO}_3^-$   
314 (Fig. 3.). For example, in Chlorophyta, specimens belonging to genera like *Caulerpa*, *Cladophora*,

315 *Codium*, *Ulva*, while in Ochrophyta,  $\delta^{13}\text{C}$  values  $>-10\text{‰}$  were recorded in genera as *Colpomenia*,  
316 *Dictyota*, *Padina*, *Sargassum*. In the case of Rhodophyta, high  $\delta^{13}\text{C}$  values were observed in  
317 calcifying macroalgae species like *Amphiroa* and *Jania* (showed in purple bars, Fig. 3c) but also in  
318 fleshy macroalgae like *Gigartina*, *Hypnea*, and *Polysiphonia*. On the contrary, values lower than -  
319  $30\text{‰}$  that denote uptake of  $\text{CO}_2$  by diffusion, were observed only in Rhodophyta in *Schizymenia*  
320 *Halymenia*, and *Gigartina*. Even so, most specimens showed  $\delta^{13}\text{C}$  signals that evidence a mechanism  
321 that uses a mix of  $\text{HCO}_3^-$  and  $\text{CO}_2$  for photosynthesis.

322 A multiple comparison analyses revealed significant differences in the  $\delta^{13}\text{C}$ -macroalgal values  
323 among genera, ordered as *Schizymenia*  $<$  *Polysiphonia*  $<$  *Ulva*, *Gracilaria* and *Spyridia* ( $-16.1\pm 0.6\text{‰}$   
324 to  $-15.1\pm 0.2\text{‰}$ )  $<$  *Gymnogongrus*, *Laurencia*, *Hypnea*, *Cladophora*, *Dictyota*, *Sargassum*,  
325 *Chaetomorpha*, and *Grateloupia* (from  $-15.4\pm 0.7\text{‰}$  to  $-13.8\pm 0.8\text{‰}$ )  $<$  *Codium* and *Padina* ( $-$   
326  $12.5\pm 2.4\text{‰}$  to  $-12.4\pm 2.5\text{‰}$ )  $<$  *Colpomenia* and *Amphiroa* ( $-9.2\pm 0.3$  to  $-7.8\pm 0.7\text{‰}$ ) ( $F=16.81$ ,  
327  $p<0.001$ ).

328 Aggrupation of  $\delta^{13}\text{C}$  values based on morpho-functional features on macroalgae is displayed in Fig.  
329 4. The most representative groups in the phylum Chlorophyta varied from  $-15.8\pm 0.3\text{‰}$  for C-Tubular  
330 to  $-12.4\pm 0.5\text{‰}$  for C-thallus erect. The phylum Ochrophyta includes O-Thick leathery with the  
331 lowest mean ( $-14.8\pm 0.3\text{‰}$ ) and O-Hollow with a spherical or subspherical shape with the highest  
332 values ( $-9.2\pm 0.3\text{‰}$ ). The lowest and highest  $\delta^{13}\text{C}$  values for Rhodophyta were observed for R-  
333 flattened macrophytes ( $-24.0 \pm 9.6\text{‰}$ ) and R-Larger-sized articulated coralline ( $-7.89\pm 0.75\text{‰}$ ),  
334 respectively. Significant differences were observed among groups, which were ordered as follows:  
335 R-flattened macrophytes  $<$  R-blade like  $<$  C-Tubular  $<$  O-Thick leathery and R-Large size corticated  $<$   
336 C-Blade like and C-Filamentous uniseriate  $<$  C-Erect thallus and O-Compressed with branch  $<$  O-  
337 Hollow with spherical  $<$  R-Larger-sized articulated coralline.

338 High intraspecific variability in  $\delta^{13}\text{C}$  signal for the more representative genera of each taxon is  
339 showed in Table 1-3. For *Codium*, *C. brandegeei* ( $11.8 \pm 1.2\text{‰}$ ) and *C. simulans* ( $-11.4 \pm 2.2\text{‰}$ )  
340 showed higher  $\delta^{13}\text{C}$  values than *C. amplivesiculatum* ( $-14.4 \pm 2.7\text{‰}$ ). *Colpomenia* species had higher  
341  $\delta^{13}\text{C}$  values than the other genera, with higher values for *C. tuberculata* ( $-8.7 \pm 3.2\text{‰}$ ) than  
342 *Colpomenia* sp. ( $-10.9 \pm 3.6\text{‰}$ ) and *C. sinuosa* ( $-10.2 \pm 2.9\text{‰}$ ). *Gracilaria* showed comparable  $\delta^{13}\text{C}$   
343 values in the four species (from  $-16.4 \pm 1.6\text{‰}$  for *G. pacifica* to  $-15.5 \pm 2.4\text{‰}$  for *Gracilaria* sp.).  
344 *Hypnea* showed non-significant  $\delta^{13}\text{C}$  differences in three representative species ( $-16.4 \pm 1.7\text{‰}$  for *H.*  
345 *spinella* to  $-14.9 \pm 2.3\text{‰}$  for *Hypnea* sp.). *Laurencia* sp. ( $-12.9 \pm 1.2\text{‰}$ ) was higher than *L. pacifica* ( $-$   
346  $14.9 \pm 2.2\text{‰}$ ), while *Padina* sp. ( $-11.1 \pm 1.5\text{‰}$ ) higher than *P. durvillaei* ( $-13.2 \pm 2.6\text{‰}$ ). *Sargassum* was  
347 one of the most diverse genera studied with six representative species, with  $\delta^{13}\text{C}$  values ordered as  
348 follow: *S. horridum* = *S. sinicola* = *S. johnstoniis* ( $-15.5 \pm 2.9$  to  $-15.1 \pm 2.4\text{‰}$ ) < *S. lapazeanum* ( $-$   
349  $14.5 \pm 1.6\text{‰}$ ) = *Sargassum* sp. ( $-14.2 \pm 2.3\text{‰}$ ) < *S. herphorizum* ( $-13.6 \pm 1.6\text{‰}$ ). *Spyridia* sp. ( $-$   
350  $17.0 \pm 1.2\text{‰}$ ) and *S. filamentosa* ( $-15.8 \pm 3.8\text{‰}$ ) showed non-significant differences. The six  
351 representative species of *Ulva* were divided into two morphological groups, filamentous and  
352 laminates. Filamentous species that averaged  $-16.3 \pm 2.0\text{‰}$  for *U. clathrata*,  $-16.0 \pm 3.6\text{‰}$  for *U.*  
353 *flexuosa*,  $-15.7 \pm 1.7\text{‰}$  for *U. acanthophora* and  $-15.3 \pm 2.5\text{‰}$  for *U. intestinalis* and *Ulva laminates*  
354 that included *U. linza* ( $-15.5 \pm 2.4\text{‰}$ ) and *U. lactuca* ( $-14.1 \pm 3.1\text{‰}$ ). Non-significant differences were  
355 observed between morphological groups and among species. A high intra-specific variability, 11-  
356 28%, explains average overlapping.

### 357 **3.3. $\delta^{13}\text{C}$ -macroalgal variability in coastal sectors**

358 Despite that, each taxon recorded a different number of genus and species along the GC coast (SI1),  
359 the macroalgal assemblages according to their fico-floristic region also express differences in their  
360 carbon uptake strategies, and their proportion inferred by their  $\delta^{13}\text{C}$  signal are shown in Fig. 5. Even



361 though most species inhabiting the GC coastal sectors displayed domination of strategies based on  
362 active CCM's, but the tendencies were different between taxa and coastal regions. The strategy that  
363 combined different sources of DIC were dominant in all regions and taxa (60-90%). Exceptions were  
364 observed in the P1 (68%) and C1 (37%) regions for Ochrophyta, where the specialized strategy of  
365 only  $\text{HCO}_3^-$  user were significant. The strategy based on only use of  $\text{CO}_2$  was observed in the  
366 peninsular coast in P2 and P3 for Rhodophyta with 2-3.3%. Overall, more negative  $\delta^{13}\text{C}$  values in  
367 macroalgae specimens' values of the same genus were observed at continental (C2) compared to  
368 peninsular coastline (P1-P3) and more negative southward than northward.

369

#### 370 **3.4. $\delta^{13}\text{C}$ -macroalgal variability in function of taxonomy and habitat features and** 371 **environmental conditions**

372 Variability of  $\delta^{13}\text{C}$  values for the most representative genera was evaluated by multiple comparative  
373 analyses in the habitat features' function, including the substrate, hydrodynamic, and emersion level.  
374 Large  $\delta^{13}\text{C}$  variability observed between specimens of the same genus collected in the different  
375 habits does not show any significant pattern, and non-significant differences were observed. An  
376 exception was observed with the emersion level (showed in Fig. 6), where intertidal specimens  
377 recorded lesser negative values than subtidal in most macroalgae genus. For example, for  
378 *Hydroclathrus* (intertidal  $-5.7 \pm 0.9\%$ ; subtidal  $-11.4 \pm 5.9\%$ ), *Amphiroa* (intertidal  $-6.9 \pm 1.5$ ; subtidal  
379  $-9.9 \pm 6.1$ ), *Hypnea* (intertidal  $-13.5 \pm 2.5\%$ ; subtidal  $-18.6 \pm 1.8\%$ ), and *Laurencia* (intertidal -  
380  $13.5 \pm 1.3\%$ ; subtidal  $-17.1 \pm 1.8\%$ ). Exceptions were observed for *Polysiphonia* (intertidal -  
381  $19.7 \pm 2.2\%$ , subtidal  $-14.9 \pm 6.7\%$ ), *Spyridia* (intertidal  $-16.9 \pm 3.3\%$ , subtidal  $-13.2 \pm 0.7\%$ ) and  
382 *Colpomenia* (intertidal  $-9.4 \pm 3.4\%$ , subtidal  $-7.7 \pm 1.3\%$ ).

383 Non-significant differences were observed for the same genera at different temperatures ranges,

384 except for *Grateloupia* (cold,  $-19.2 \pm 4.7\text{‰}$ , typical  $-14.4 \pm 2.2\text{‰}$ , warm  $-14.5 \pm 2.2\text{‰}$ ) and  
385 *Polysiphonia* (cold,  $-21.0 \pm 0.4\text{‰}$ , typical  $-18.1 \pm 5.5\text{‰}$ , warm  $-17.9 \pm 2.3\text{‰}$ ) with more negative values  
386 in colder than warmer waters ( $F=6.42$ ,  $p<0.001$ ). Neither significant difference was observed in  $\delta^{13}\text{C}$   
387 values in macroalgae specimens from the different genus in the same temperature range. For  
388 example, *Colpomenia* (cold  $-8.3 \pm 2.4\text{‰}$ , typical  $-9.4 \pm 3.7\text{‰}$ , warm  $-9.2 \pm 2.6\text{‰}$ ), *Codium* (cold -  
389  $11.9 \pm 1.9\text{‰}$ , typical  $-12.5 \pm 3.0\text{‰}$ , warm  $-13.6 \pm 0.6\text{‰}$ ), and *Padina* (cold  $-11.3 \pm 2.5\text{‰}$ , typical -  
390  $11.8 \pm 1.7\text{‰}$ , warm  $-13.4 \pm 2.7\text{‰}$ ) (Fig. 7a).

391 Significant differences were observed among genus related to the pH level at seawater (Fig. 7b).  
392 Under typical pH seawater, *Amphiroa* and *Colpomenia* were 1-2‰ more negatives than in alkaline  
393 waters, while *Ulva* and *Spyridia* were 3-5‰ less negative than in acidic waters. *Amphiroa* and  
394 *Colpomenia* were not collected in acidic water, and neither *Spyridia* in alkaline waters to compare.  
395 Another genus also showed extremes values between alkaline (*Tacanoosca*  $-7.6 \pm 1.0\text{‰}$ ) and acidic  
396 waters (*Schizymenia*,  $-32.9 \pm 2.0\text{‰}$ ). The following order was observed in the genus collect at the  
397 three pH ranges: alkaline > typical > acidic. Significant differences were observed for genus  
398 *Ahnfeltiopsis*, *Caulerpa*, *Gymnogongrus*, *Padina*, and *Ulva*, with higher values at alkaline than in  
399 acidic waters. Values of  $\delta^{13}\text{C}$  for specimens of the same genus collected at typical pH waters are  
400 mostly overlapped between those for alkaline and acidic seawaters. Non-significant differences in  
401  $\delta^{13}\text{C}$  values were observed for *Grateloupia*, *Hypnea*, and *Polysiphonia* concerning pH-type waters.

402 We analyzed the carbon uptake strategies on macroalgal assemblages in the function of  
403 environmental factors like temperature, pH, and salinity (Fig. 8). Regarding the  $\delta^{13}\text{C}$  variability for  
404 all data set in response to temperature and salinity, non-significant trend was observed between  $\delta^{13}\text{C}$ -  
405 macroalgal in both parameters' function. A poor but significant correlation was observed between  
406  $\delta^{13}\text{C}$  and pH ( $R^2 = 0.04$ ) (Table 4). The proportion of specimens with a strategy of only  $\text{HCO}_3^-$  use

407 was different between environmental factors and taxa (previously described), for example,  
408 Ochrophyta showed the highest proportion (35%) in colder temperature, in pH-Alkaline (31%), and  
409 at typical salinity regimen (27%), while Chlorophyta enhanced to 30% in acid pH and Rhodophyta  
410 recorded 21% at normal seawater. The opposite strategy (only use of dissolved CO<sub>2</sub>) that was  
411 observed only in Rhodophyta, the highest percentage was observed in estuarine salinity regimen  
412 (10%).

### 413 **3.5. Variation latitudinal of $\delta^{13}\text{C}$ -macroalgal**

414 The  $\delta^{13}\text{C}$ -macroalgal variation in the GC biogeography was evaluated by regression linear analysis  
415 between  $\delta^{13}\text{C}$  values along the nine degrees latitude in both GC coastlines. A non-significant  
416 latitudinal trend was observed for datasets, but for the three taxa's most representative genera,  $\delta^{13}\text{C}$   
417 values correlated with latitude (Fig. 9). In Chlorophyta, with the higher genera number,  $\delta^{13}\text{C}$  values  
418 increased with latitude, with low but significant correlation. Contrarily, in Ochrophyta and  
419 Rhodophyta specimens, the  $\delta^{13}\text{C}$  values decreased non-significantly with latitude.

420 Significant correlations ( $p < 0.001$ ) were observed for  $\delta^{13}\text{C}$ -macroalgal *versus* latitude in the most  
421 representative morphofunctional groups (Fig. 10). Representative morphofunctional groups of  
422 Chlorophyta (e.g., C-Tubular, C-Filamentous uniseriate), showed a positive correlation, while those  
423 belonging to Ochrophyta (e.g., O-thick leathery;) and Rhodophyta (e.g., R-large sized corticated)  
424 showed a negative trend with latitude.

### 425 **3.6. Analyses of $\delta^{13}\text{C}$ macroalgal variability**

426 An analysis of the effects, independent and combined, on the  $\delta^{13}\text{C}$ -macroalgal variability related to  
427 life form and environmental factors, was conducted. Firstly, simple linear regression analyses were  
428 performed to evaluate the dependent variable's prediction power ( $\delta^{13}\text{C}$ -macroalgal) in the function

429 of several independent variables controlling the main macroalgae photosynthesis drivers (light, DIC,  
430 and inorganic nutrients). Regression coefficients were estimated for each fitted regression model,  
431 which is used as indicators of the quality of the regression (Draper and Smith, 1998; Burnham and  
432 Anderson, 2002) as was described in Methods; however, our results description focused on the  
433 coefficients of determination ( $R^2$  and adjusted  $R^2$ ). The coefficient  $R^2$  describes the overall  
434 relationship between the independent variables  $X_i$  with the dependent variable  $Y$  ( $\delta^{13}\text{C}$ -macroalgal),  
435 and it is interpreted as the % of contribution to the  $\delta^{13}\text{C}$  variability. While the adjusted  $R^2$  statistics  
436 compensate for possible confounding effects between variables.

437 Results of the analysis of the relationships between  $\delta^{13}\text{C}$  with each independent variable are  
438 summarized in Table 4. Regarding the inherent macroalgae properties, Phyla explain only 8%  
439 variability, the morphofunctional properties 35%, and taxon by genus 46%, and by species 57%.

440 The biogeographical collection zone, in terms of coastline (continental vs. peninsular) and coastal  
441 sectors (C1-C3 and P1-P3), explained a maximum of 5% variability. Related to the habitat features,  
442 only the emersion level (6%) contributed to the  $\delta^{13}\text{C}$  variability. The contribution of the seawater's  
443 environmental conditions was marginal for pH (4%) and negligible for temperature and salinity. A  
444 marginal reduction in the percentage of contribution was observed for Phyla (1%) and  
445 morphofunctional properties (1%), but significant for genus (5%) and species (10%).

446 Multiple regression analyses were also performed to interpret the complex relationships among  $\delta^{13}\text{C}$ -  
447 macroalgal, considering the life form (morphofunctional and taxon by genus) and their responses to  
448 environmental parameters. Results for the fitted regression models performed for morphofunctional  
449 groups (Table 5) and genus (Table 6) evidenced that the effect of the coastal sector and pH ranges  
450 on the  $\delta^{13}\text{C}$ -macroalgal increased the contribution by 9-10% each one. The emersion level increased  
451 by 5-6%, the contribution respect to individual effect of morphofunctional group and genus, the

452 temperature and pH in 1 and 3%, respectively, while salinity decreased by 1-2%. Adding the effect  
453 of the biogeographical collection zone, represented by the coastline sector, to those for  
454 morphofunctional group (Table 5) and genus (Table 7), a notable increase of 11-12% was observed.  
455 The full model considering the combined effect of the coastline sector + Habitats features for  
456 Morphofunctional group or Genus (Table 7), showed  $R^2$  of 0.60 and 0.71. In contrast, Coastline  
457 sector + Environmental conditions + Morphofunctional group or Genus the  $R^2$  increased to 0.62 and  
458 0.72, respectively. The interactive explanations of environmental factors increased the explanation  
459 percentage of  $\delta^{13}\text{C}$  variability; however, these contributions were significantly lower than the  
460 explained by life forms, such as the morphofunctional properties and taxa by genus and species.  
461 The combined effect of environmental condition on the  $\delta^{13}\text{C}$  variability was tested for the best-  
462 represented morphological groups and genus. Results evidenced that 9 of 21 morphological groups  
463 showed significant effects on the  $\delta^{13}\text{C}$  variability (Table 8), five increasing and four decreasing the  
464 model constant of  $\delta^{13}\text{C} = -14.2\text{‰}$ . For example, for the O-Hollow with spherical or subspherical shape  
465 (+4.9‰) and R-Larger-sized articulated corallines (+6.3‰), the predicted values are  $-7.9 \pm 0.8\text{‰}$  and  
466  $-9.2 \pm 0.4\text{‰}$ . For R-Filamentous uniseriate and pluriseriate with erect thallus (-2.1‰) and C-Tubular  
467 (-1.6‰), the predicted values are  $-16.3 \pm 0.5\text{‰}$  and  $-15.8 \pm 0.5\text{‰}$ , respectively. Regarding taxon, a  
468 significant effect was observed only in 13 genera, including *Colpomenia* (+5.4‰), *Amphiroa*  
469 (+6.8‰), and *Padina* (+2.2‰) increasing the signal, and *Polysiphonia* (-3.7‰), *Gracilaria* (-0.9‰),  
470 and *Spyridia* (-1.4‰) decreasing the signal of the model constant (Table 9). In 33 species was  
471 observed a significant effect on the  $\delta^{13}\text{C}$  variability, including *C. tuberculata* +5.9‰, *C. sinuosa*  
472 +4.4‰, *H. pannosa* +4.4‰, *H. johnstonii* +4.4‰, and *Amphiroa* spp. (+4.4 to 8.2‰) increasing the  
473 model constant  $\delta^{13}\text{C} = -14.6\text{‰}$ , and *Spyridia* sp. (-2.5‰), *G. filicina* (-2.3‰), *P. mollis* (-5.2‰) and  
474 *S. pacifica* (-19.2‰) (Table 10).

475

### 476 **3.7. Preliminary estimations of $\Delta^{13}\text{C}$ -macroalgal**

477 Concurrent analysis of surface seawater for alkalinity, proportions of the chemical species of DIC  
478 ( $\text{CO}_2$ ,  $\text{HCO}_3^-$ , and  $\text{CO}_3^{2-}$ ), and  $\delta^{13}\text{C}$ -DIC evidenced that  $\delta^{13}\text{C}$ -DIC in GC seawater averages  
479  $1.4 \pm 0.4\text{‰}$  (-1 to  $4.9\text{‰}$ ) (Fig. S1). In our preliminary data, the  $\delta^{13}\text{C}$ -DIC seawater slightly (in  $0.5\text{‰}$ )  
480 decreased during the rainy season in those zones influenced by river discharges along the continental  
481 coastline, with non-significant differences among coastal sectors.  $\delta^{13}\text{C}$ -DIC values in GC seawater  
482 are comparable to the averages  $1.4$ - $1.6\text{‰}$  reported for the surface seawaters in the Eastern North  
483 Pacific in the 1970s-2000s period (Quay et al., 2003; Hinger et al., 2010; Santos et al., 2011).

484 Based on the subtraction of  $\delta^{13}\text{C}$  macroalgae to  $\delta^{13}\text{C}$ -DIC seawater, the integrative discrimination  
485 factor against  $^{13}\text{C}$  averaged  $16.0 \pm 3.1\text{‰}$ ,  $16.8 \pm 4.3\text{‰}$ , and  $14.0 \pm 3.8\text{‰}$  for Phyla Chlorophyta,  
486 Rhodophyta, and Ochrophyta, respectively. Five groups were identified in function of the  $\Delta^{13}\text{C}$   
487 values, one for Chlorophyta ( $\Delta^{13}\text{C} = 16.0 \pm 3.1\text{‰}$ ), two for Rhodophyta ( $16.6 \pm 3.8\text{‰}$  and  $34.6 \pm 1\text{‰}$ ),  
488 and two for Ochrophyta ( $9.1 \pm 1.7\text{‰}$  and  $15.7 \pm 2.7\text{‰}$ ) (Fig. S2). Values of  $\Delta^{13}\text{C}$  were comparable to  
489  $\delta^{13}\text{C}$  of the thallus of macroalgae, thus  $\delta^{13}\text{C}$ -macroalgal reflect mainly the discrimination during  
490 carbon assimilation. Like  $\delta^{13}\text{C}$ -macroalgal, the  $\Delta^{13}\text{C}$  values were subject to considerable variation.

491

## 492 **4. Discussions**

### 493 **4.1. Explaining the $\delta^{13}\text{C}$ macroalgal variability**

494 In this study, results revealed high variability in the  $\delta^{13}\text{C}$  of the large inventory of macroalgae  
495 collected along GC coastline between five years period. A linear regression analysis of the effects  
496 of life form revealed that the  $\delta^{13}\text{C}$ -macroalgal variability is mainly explained by taxonomic (genus

497 46%, species 57%) and morphofunctional groups. This result is consistent with the report of  
498 Lovelock et al., (2020), who found that 66% of  $\delta^{13}\text{C}$  variability was explained by taxonomy. Even  
499 so, the variability associated with each genus is not the same and can be classified in three groups:  
500 1) high variability (e.g., *Schizymenia*  $=\pm 19.1\%$ ), moderate variability (e.g., *Hydroclathrus*  $=\pm 7.3\%$ ;  
501 *Amphiroa*  $=\pm 6.8\%$ ) and low variability (e.g., *Gracilaria*  $=\pm 0.89$ ; *Spyridia*  $=\pm 1.46\%$ ).

502 Most authors studying the isotopic composition of C in macroalgae have reported the high isotopic  
503 variability, which has been attributable to the taxon-specific photosynthetic DIC acquisition  
504 properties (Raven et al., 2002a, Mercado et al., 2009, Marconi et al., 2011, Stepien, 2015, Díaz-  
505 Pulido et al., 2016; Lovelock et al., 2020). In our study, we observed that the intrinsic characteristics  
506 of each morpho-functional group of macroalgae (e.g., thallus structure, growth form, branching  
507 pattern, and taxonomic affinities) are determinant of the  $\delta^{13}\text{C}$ -macroalgal signals. Although non-  
508 evaluated in this study, the maturity of the specimens (e.g., young, adult, vs senescence) is also  
509 relevant (e.g., Carvalho et al., 2007; 2009b).

510 The  $\delta^{13}\text{C}$ -macroalgal depends on the carbon source ( $\delta^{13}\text{C}$ -DIC in seawater), the isotope  
511 discrimination during carbon assimilation in the photosynthesis ( $\Delta^{13}\text{C}_p < 29\%$  in a variable degree),  
512 and the plant respiration ( $\Delta^{13}\text{C}_r$  average  $\pm 2.3\%$ ) (Carvalho et al., 2009a,b, 2010; Carvalho and Eyre,  
513 2011, Rautemberger et al., 2015). Comparatively, the  $\Delta^{13}\text{C}_r$  value is relatively small regarding  $\Delta^{13}\text{C}_p$ ,  
514 thus  $\delta^{13}\text{C}$ -macroalgal basically is an integrative value of the isotope discrimination during  
515 DICseawater assimilation [ $\Delta^{13}\text{C} = (\delta^{13}\text{C}\text{-DIC seawater} - \delta^{13}\text{C}\text{macroalgae})$ ] (Carvalho et al., 2009a).  
516 Based on the  $\Delta^{13}\text{C}$  values, five groups were identified in our study: one for Chlorophyta  
517 ( $\Delta^{13}\text{C} = 16.0 \pm 3.1\%$ ), two for Rhodophyta ( $16.6 \pm 3.8\%$  and  $34.6 \pm 1\%$ ), and two for Ochrophyta  
518 ( $9.1 \pm 1.7\%$  and  $15.7 \pm 2.7\%$ ). Values of  $\Delta^{13}\text{C}$  were comparable to  $\delta^{13}\text{C}$  of the thallus of macroalgae,  
519 thus  $\delta^{13}\text{C}$ -macroalgal reflect mainly the discrimination during carbon assimilation. The  $\delta^{13}\text{C}$ -

520 macroalgal values reflect the discrimination during carbon assimilation attributable to the taxon-  
521 specific photosynthetic DIC acquisition properties.  $\Delta^{13}\text{C}$ -macroalgal variability, captured in the  $\delta^{13}\text{C}$ -  
522 macroalgal signals, is related to thickness of the boundary layer around the thallus (Raven et al.  
523 1982), the leakage during carbon uptake (Sharkey and Berry 1985, Maberly et al. 1992), and  
524 photosynthetic intensity (Wiencke and Fischer 1990, Kübler and Raven 1994, 1995), and respiration  
525 rates (Carvalho et al., 2010; Carvalho and Eyre, 2011, Rautemberger et al., 2015). All intrinsic  
526 properties related to the life form.

527 Many species that recorded high  $\delta^{13}\text{C}$  values (and low  $\Delta^{13}\text{C}$  values) were fleshy macroalgae that are  
528 characterized to be bloom-forming macroalgae belonging to genera *Ulva*, *Gracilaria*, *Cladophora*,  
529 *Spyridia*, and *Sargassum* (Páez-Osuna et al., 2013, Valiela et al., 2018). It is not surprising, due to  
530 species with high photosynthetic activity and high relative growth rates (Hiraoka et al., 2020) have  
531 high carbon demand that results in lower isotopic discrimination against  $^{13}\text{C}$  (Cornelisen, et al., 2007;  
532 Carvalho et al., 2010ab; Kübler and Dungeon, 2015; Rautemberger et al., 2015). Bloom-forming  
533 macroalgae (e.g., *Ulva*, *Gracilaria*, *Sargassum*) have been remarks as facultative species with the  
534 capacity to switch from C3 to C4 pathway (Valiela et al., 2018). C4 pathway reduces  
535 photorespiration, the antagonist process of RuBisCo, enhancing the DIC assimilation in 25-40% and  
536 increasing the  $\delta^{13}\text{C}$  values (Ehleringer et al., 1991; Bauwe et al., 2010; Zabaleta et al., 2012). C4  
537 pathway has more energy investment in CCM's than in RuBisCo protein content than C3 pathway  
538 (Young et al., 2016). Also, the reports of features of C4 or C4-like pathway in algae have increased  
539 in the last years (Roberts et al., 2007; Doubnerová and Ryslavá, 2011; Xu et al., 2012, 2013). For  
540 example, high activity of keys enzymes of C4 metabolisms, such as pyruvate orthophosphate  
541 dikinase (PPDK), phosphoenolpyruvate carboxylase (PEPC), and phosphoenolpyruvate  
542 carboxykinase (PCK), has been described in many algae species. But the establishment of a true C4



543 pathway in marine algae is not clear since the massive changes in gene expression patterns seem to  
544 be incomplete, and it is suggested that many marine algae have high plasticity to use a combination  
545 of CCM to overcome  $C_i$  limitations (Roberts et al., 2007; Doubnerová and Ryslavá, 2011; Xu et al.,  
546 2012, 2013). A Stepwise model of the path from  $C_3$  to  $C_4$  photosynthesis is explained by Gowik and  
547 Westhoff (2011). More research is required on this topic considering the increasing the frequency,  
548 intensity, and extension of bloom-forming macroalgae events worldwide (Teichberg et al., 2010;  
549 Valiela et al., 2018) and in México (Ochoa-Izaguirre et al. 2007; Ochoa-Izaguirre and Soto-Jiménez  
550 2015; Páez-Osuna et al., 2017).

551 Changes in the habitat features and environmental conditions, such as light intensity and DIC  
552 availability, influencing the growth rate and photosynthetic intensity, have a strong influence on  $\delta^{13}C$   
553 signal (Carvalho et al., 2007, 2009; Carvalho and Eyre, 2011; Stepien, 2015; Mackey et al., 2015;  
554 Rautenberger et al., 2015). The light intensity is the external factor with more influence on the  $\Delta^{13}C$ -  
555 macroalgal due to the regulation of carbon assimilation intensity (Wefer and Killingley 1986, Cooper  
556 and DeNiro 1989, Grice et al. 1996; Carvalho et al., 2009a,b). Experimental studies found the light  
557 levels as a key factor affecting the  $\delta^{13}C$  values, for example under saturating light conditions *Ulva*  
558 switched from a carbon uptake of  $HCO_3^-$  and  $CO_2$  to increased  $HCO_3^-$  use (Rautemberger et al.,  
559 2015). Furthermore, field studies have shown that species growing in low light habitats as deep  
560 subtidal tend to have more negative  $\delta^{13}C$  values than those in higher light environments (Mercado et  
561 al., 2009; Hepburn et al., 2011; Marconi et al., 2011; Stepien 2015; Cornwall et al., 2015, Díaz-  
562 Pulido et al., 2016). In this study, intertidal specimens recorded lesser negative values than subtidal  
563 in most macroalgae genus. However, the vertical effect in the  $\delta^{13}C$  signal related to the light  
564 limitation was not recorded in our study because only shallow habitats (non-light limited), were  
565 considered.

566  $\delta^{13}\text{C}$ -DICseawater is reasonably uniform in surface seawater (-4.8 to 3.6‰, median 1.5‰), with  
567  $\delta^{13}\text{C}$  values for  $\text{CO}_2$ ,  $\text{HCO}_3^-$ , and  $\text{CO}_3^{2-}$  nearly -10, -0.5 and 2‰, respectively (Mook et al., 1974;  
568 Kroopnick 1985). Exceptions can be expected where variations in the salinity, alkalinity, and  
569 proportions of the chemical species of DIC ( $\text{CO}_2$ ,  $\text{HCO}_3^-$  or  $\text{CO}_3^{2-}$ ) occur (e.g., in coastal  
570 environments influenced by river and groundwater discharges) (Mook et al., 1974; Chanton and  
571 Lewis 1999; Hinger et al., 2010; Carvalho et al., 2015). Regarding DIC sources for macroalgae in  
572 the GC surface seawater, the availability, chemical proportions and  $\delta^{13}\text{C}$ -DIC, were also relatively  
573 constant and uniform. Thus, the influence of the  $\delta^{13}\text{C}$ -DIC variations to the  $\delta^{13}\text{C}$ -macroalgal  
574 variability is negligible in the GC.

575 The effect of other environmental factors, such as salinity and pH, on  $\delta^{13}\text{C}$ -macroalgal signals were  
576 evaluated. Regarding salinity, the influence of freshwater discharge by rivers and groundwater  
577 decreases the  $\delta^{13}\text{C}$  signal, which could be explained by the effect of the reduction in the salinity  
578 regimen that follows a decrease in  $\delta^{13}\text{C}$ -DIC in water (Hinger et al., 2010; Santos et al., 2011). In  
579 our study, non-significant correlation between  $\delta^{13}\text{C}$ -macroalgal and salinity was observed.

580 Based on pH, differences in  $\delta^{13}\text{C}$  were found only for a few genera (e.g., *Amphiroa*, *Colpomenia*,  
581 *Ulva*, *Spyridia*), with a trend to increase in the  $\delta^{13}\text{C}$  values with pH increase, such as was reported  
582 by Maberly et al. (1992) and Raven et al. (2002b). Similar results were reported for Cornwall et al.  
583 (2017) in the field study, with the differential response of the  $\delta^{13}\text{C}$  signals to pH among 19 species,  
584 in which only four species were sensitive to pH changes. Based on the complete dataset, a very weak  
585 but significant positive linear regression was observed between  $\delta^{13}\text{C}$  and pH. Also, a trend to  
586 decrease in the  $\delta^{13}\text{C}$  was recorded in the follow order: alkaline > typical > acidic. According to  
587 Stepien (2015), the result of meta-analyzes between pH values and  $\delta^{13}\text{C}$  was positive only for  
588 Rhodophyta and Ochrophyte, but not for Chlorophyta. About 86% of the Stepien metadata met the

589 theoretical CCM assignation based on both parameters, exceptions for species with  $\delta^{13}\text{C} < -30\text{‰}$  that  
590 have been capable of raising  $\text{pH} > 9$ . A strong association between  $\text{pH}$  compensation point and  $\delta^{13}\text{C}$   
591 was reported by Iñiguez et al. (2009) in three taxa of polar macroalgae.

#### 592 **4.2. Using $\delta^{13}\text{C}$ -macroalgal to infer carbon uptake strategies**

593 In our study, the  $\delta^{13}\text{C}$  signal from the thallus of macroalgae was used to infer carbon strategies. This  
594 tool was first used in macroalgal shallows communities of the Gulf of California. Most macroalgae  
595 species displayed  $\delta^{13}\text{C}$  values that exhibit an active CCM's. About of 84% of the total analyzed  
596 specimens showed the facultative uptake of  $\text{HCO}_3^-$  and  $\text{CO}_2$ , the most common strategy identified  
597 in macroalgal shallow communities (Hepburn et al., 2011; Cornwall et al., 2015; Stepien 2015; Díaz-  
598 Pulido et al., 2016). Based on the carbon uptake strategies, the most abundant macroalgae were those  
599 able to use both  $\text{HCO}_3^-$  and/or  $\text{CO}_2$  by means of active uptake plus passive diffusion (strategy 2: -  
600  $10 < \delta^{13}\text{C} > -30\text{‰}$ ).

601 Macroalgae collected in GC also involved those that are only  $\text{HCO}_3^-$  users (strategy 1:  $\delta^{13}\text{C} > -10\text{‰}$ )  
602 and those relying on diffusive  $\text{CO}_2$  uptake (strategy 3:  $\delta^{13}\text{C} < -30\text{‰}$ ). Photosynthesis that relies on  
603  $\text{CO}_2$  uptake (lack of CMM), the most primitive mechanism (Cerling et al., 1993), has fewer energy  
604 costs than  $\text{HCO}_3^-$  uptake that requires complex machinery with a high operational cost (Giordano et  
605 al., 2005; Hopkinson et al., 2011; Hopkinson, 2014; Raven and Beardall, 2016). The energy for  
606 macroalgae to uptake  $\text{HCO}_3^-$ , cross the plasma membrane, and covert to  $\text{CO}_2$  for photosynthesis, is  
607 obtained through irradiance (Cornelisen et al., 2007). Based on our sampling effort, focused on  
608 intertidal and shallow subtidal habitats featured by high-light intensities, we expected high  
609 proportions of species and specimens with the carbon uptake strategy that use only  $\text{HCO}_3^-$ . Results  
610 evidenced that strategy 1 was recorded in specimens belonging to 58 species of 170 total species.

611 The higher proportions of CCM species ( $\text{HCO}_3^-$  users), with high-energetic requirements, is  
612 explained by those elevated irradiances (Hepburn et al. 2011; Cornwall et al. 2015). Ochrophyta  
613 showed the highest proportion of species and specimens that depend only on  $\text{HCO}_3^-$  uptake on both  
614 coastlines in the southern region of GC (P1, C1). These differences can be partially explained by the  
615 low solubility of  $\text{CO}_2$  due to relatively high temperatures in subtropical waters (Zeebe and Wolf-  
616 Gladrow, 2007) that impulse the development of CCM (Raven et al., 2002b) and by the high affinity  
617 to DIC by Ochrophyta, such as has been described before by Diaz-Pulido et al, (2016).

618 Only three non-calcifying species (*Schizymenia pacifica*, *Halymenia* sp., *Gigartina* sp.) belonging  
619 to Rhodophyta were  $\text{CO}_2$  exclusive users ( $\delta^{13}\text{C}=-33.2\pm 1\text{‰}$ ). Based on measurements of pH drift,  
620 Murru and Sandgreen (2004), reported to *Schizymenia pacifica* and two species of *Halymenia* (e.g.,  
621 *H. schizymenioides* and *H. gardner*) as restricted  $\text{CO}_2$  users. Measurements of  $\delta^{13}\text{C}$  in *Halymenia*  
622 *dilatate* confirmed the  $\text{CO}_2$ -restricted photosynthesis in specimens collected offshore in deep reefs  
623 of the Great Barrier reef (Díaz-Pulido et al., 2016). Red macroalgae that lack CCM, tend to inhabit  
624 low-light habitats like subtidal or low intertidal and are abundant in cold waters (Kübler et al., 1999,  
625 Raven et al., 2002a, Cornwall et al., 2015). According to these authors, approximately 35% of the  
626 total red algae tested on a global scale are strictly  $\text{CO}_2$  dependents. The percentage of macroalgae  
627 species representative of Arctic and Antarctic ecosystems that lack CCM is 42-60% (Raven et al.,  
628 2002b; Iñiguez et al., 2019), 50% for temperate waters of New Zealand (Hepburn et al., 2011), and  
629 up to 90% found for a single site of Tasmania Australia (Cornwall et al., 2015). In our study, 91 red  
630 macroalgae species were sampled (of 453 red macroalgae species reported in the GC, Pedroche and  
631 Senties, 2003), of which <3% were  $\text{CO}_2$  dependents. This low percentage could be related to the fact  
632 that deep habitats (>2 m depth low tide) were not explored in our surveys.

633 In our study, few calcifying macroalgae species using  $\text{HCO}_3^-$  and diffusive  $\text{CO}_2$  (strategy 4) were

634 also collected, including the genera *Amphiroa* ( $-7.8\pm 3.7\%$ ) and *Jania* ( $-9.4\pm 0.7\%$ ), both  
635 Rhodophyta with articulated-form. *Padina*, a genus with less capacity to precipitate  $\text{CaCO}_3$  (Ilus et  
636 al., 2017), displayed relatively high  $\delta^{13}\text{C}$  values ( $-12.5\pm 2.4\%$ ) suggesting the presence of CCM using  
637  $\text{HCO}_3^-$  exclusively. Three genera are very common in the GC. Stepien (2015) reported a global mean  
638 of  $-14.8\pm 1.0\%$  for calcifying species compared to  $-20.1\pm 0.3\%$  for non-calcifying species. Calcifying  
639 species have a different carbon uptake strategy influenced by the calcifying process that results in  
640 elevated  $\delta^{13}\text{C}$  signals (Diaz-Pulido et al., 2016). High  $\delta^{13}\text{C}$  values for calcifying species are related  
641 to the excess of  $\text{H}^+$  released as residuals products of the calcifying process, also the acidified  
642 boundary layers benefit the  $\text{HCO}_3^-$  uptake (McConnaughey and Whelan 1997, Courneau et al.,  
643 2012). The high  $\delta^{13}\text{C}$  values can also be related to the highly efficient light properties that are  
644 enhanced by the carbonate skeleton, resulting in an optimization of photosynthetic activity (Vasquez-  
645 Elizondo et al., 2017). Hofmann and Heesch (2018) reported high  $\delta^{13}\text{C}$  values in eight rhodoliths  
646 species (calcifying species) for the organic matter thallus and thallus including  $\text{CaCO}_3$  structure  
647 collected in deep habitats (25-40 m) where light availability is very low. Because the ocean  
648 acidification in progress, negative impacts are expected on calcifying organisms, more attention as  
649 ecological sentinels is warranted in the GC.

650 Based on the  $\delta^{13}\text{C}$  values, it is possible to assume that at least one basal CCM is active, however, it  
651 is impossible to discern what type of CCM is expressed in the organisms (e.g., direct  $\text{HCO}_3^-$  uptake  
652 by the anion-exchange protein AE; Drechsler and Beer 1991; Drechsler et al. 1993) or types of  
653 mitochondrial carbonic anhydrase (e.g., internal and external) that enhance the fixation of  $\text{C}_i$  by  
654 recycling mitochondrial  $\text{CO}_2$  (Bowes, 1969; Zabaleta et al., 2012; Jensen et al., 2020). Also, the co-  
655 existence of different CCMs has been described for the same species (Axelsson et al., 1999, Xu et  
656 al., 2012), even that different CCM's can operate simultaneously, generating different  $\text{C}_i$

657 contribution to RuBisCo internal pool (Rautemberger et al., 2015). The variety of CCMs and their  
658 combinations could contribute to the high  $\delta^{13}\text{C}$  variability for the same species. In our field study, it  
659 is impossible to explain the variations of  $\delta^{13}\text{C}$  or  $\Delta^{13}\text{C}$ -macroalgal relative to CCM or CA activity  
660 types. Controlled experiments, as those conducted by Carvalho and collaborators (e.g., Carvalho et  
661 al 2009a,b, 2010), are required to obtain this knowledge.

#### 662 **4.3. Variability of $\delta^{13}\text{C}$ macroalgal between the GC bioregions**

663 Changes in the  $\delta^{13}\text{C}$  signal with latitude, mainly related to the light and temperature, have been  
664 reported in the literature (Mercado et al., 2009; Marconi et al., 2011; Stepien, 2015; Hofmann and  
665 Heesch, 2018; Lovelock et al., 2020). For example, a negative correlation between latitude and  $\delta^{13}\text{C}$ -  
666 macroalgal was described by Stepien (2015), concluding that the  $\delta^{13}\text{C}$  signal increased by 0.09‰ for  
667 each latitude degree from the Equator. Hofmann and Heesch (2018) recently showed a strong  
668 decrease in latitudinal effect ( $R^2= 0.43$   $\delta^{13}\text{C}_{\text{total}}$  and 0.13, for  $\delta^{13}\text{C}_{\text{organic-tissue}}$ ,  $p=0.001$ ) for rhodolite  
669 of the northern hemisphere and macroalgae from coral reefs in Australia. In both cases, the latitude  
670 range is higher than we tested ( $30^\circ$  to  $80^\circ$  and from  $10^\circ$  to  $45^\circ$ , respectively). These differences on a  
671 big scale tend to be associated with a temperature effect (Stepien, 2015) and their effect on  $\text{CO}_2$   
672 solubility in seawater (Zeebe and Wolf-Gladrow, 2007). However, in our study, any geographical  
673 pattern in the  $\delta^{13}\text{C}$  macroalgal was observed. Our linear regression analyzes for latitudes showed a  
674 low but significant correlation for the dataset classified by morphofunctional groups and genus,  
675 negative in the cases of Rhodophyta and Ochrophyta groups, and positive for Chlorophyta.

676 Non-defined patterns may be explained by non-significant variations in light and temperature along  
677 the GC latitudes. In fact, most of the shallow habitats occupied by macroalgal communities in the  
678 GC were high-light environments with narrow ranges in temperature. However, the combined effect

679 of the coastline sector, habitats feature, or environmental condition for Morphofunctional group or  
680 Genus explained 60-62 and 71-72% of the  $\delta^{13}\text{C}$  variability, respectively. Life forms, such as the  
681 morphofunctional properties and taxa by genus and species, constitute the main contributors to the  
682 variability. Our analysis of variability for the best-represented morphological groups (e.g., R-  
683 Filamentous uniseriate and pluriseriate with erect thallus and C-Tubular) and genus (e.g.,  
684 *Colpomenia*, *Padina*, *Polysiphonia* and *Gracilaria*) revealed that certain life forms are better  
685 monitors explaining the variability of  $\delta^{13}\text{C}$ -macroalgal (and  $\Delta^{13}\text{C}$  values) than others. However, more  
686 research is required to better interpretation to evaluate the isotope discrimination during carbon  
687 assimilation and respiration across the macroalgae lifecycle.

688 The proportion of specimens with different carbon uptake strategies also showed regional variations.  
689 For example, the facultative uptake of  $\text{HCO}_3^-$  and  $\text{CO}_2$  was dominant in the macroalgal shallow  
690 communities in the GC (60 to 90% of specimens), with an exception in the P1 region for Ochrophyta  
691 where the specialized strategy of only  $\text{HCO}_3^-$  use dominated (68%), and high proportion were  
692 observed in C1 with 37%. While the strategy based on only use of  $\text{CO}_2$  was observed in the  
693 peninsular coast in P2 and P3 for Rhodophyta with 2-3.3%. Finally, the coastal sector C2 showed  
694 more negative  $\delta^{13}\text{C}$  values in macroalgae specimens of the same genus compared to peninsular  
695 coastline (P1-P3). Small but detectable changes were observed in the Phyla distribution based on  
696 environmental conditions. For example, Ochrophyta showed the highest proportion (35%) in colder  
697 temperature, in pH-Alkaline (31%), and at typical salinity regimen (27%), while Chlorophyta  
698 enhanced to 30% in acid pH and Rhodophyta recorded 21% at normal seawater. The opposite  
699 strategy (only use of dissolved  $\text{CO}_2$ ) that was observed only in Rhodophyta, the highest percentage  
700 was observed in estuarine salinity regimen (10%). Again, more research is required to obtain useful  
701 information on the physiological and environmental status of macroalgae.

## 702 5. Conclusions

703 In conclusion, we observed high  $\delta^{13}\text{C}$ -macroalgal variability in macroalgae communities in the Gulf  
704 of California, such as has been reported in other worldwide marine ecosystems. Life form is the  
705 principal cause of  $\delta^{13}\text{C}$ -macroalgal variability, and taxonomy and morphology explain up to 57%  
706 and 35% of the variability, respectively. Changes in habitat characteristics and environmental  
707 conditions also influence the  $\delta^{13}\text{C}$ -macroalgal variability. The full model considering the combined  
708 effect of the life form, coastline sector, and environmental conditions explains up to 62%  
709 (morphological groups) and 72% (genus) of the variability. The effect of the coastal sector, pH  
710 ranges, and emersion level were significant, while for salinity and temperature negligible.

711 Most macroalgae inhabiting in GC displayed the presence of  $\text{CO}_2$  carbon mechanisms to uptake  
712  $\text{HCO}_3^-$  for photosynthesis, 84% of the total analyzed specimens were able to use both  $\text{HCO}_3^-$  and/or  
713  $\text{CO}_2$  employing active uptake plus passive diffusion (strategy 2:  $-10 < \delta^{13}\text{C} > -30\text{‰}$ ). Specimens  
714 belonging to 58 species of 170 total species showed carbon uptake strategy 1 that use only  $\text{HCO}_3^-$ .  
715 A higher proportion of CCM species ( $\text{HCO}_3^-$  users) was expected because we focused on intertidal  
716 and shallow subtidal habitats featured by high-light intensities. Only three non-calcifying species  
717 (*Schizymenia pacifica*, *Halymenia* sp., *Gigartina* sp.) belonging to Rhodophyta (3%) were  $\text{CO}_2$   
718 exclusive users (strategy 3:  $\delta^{13}\text{C} < -30\text{‰}$ ). The low percentage of  $\text{CO}_2$  dependents versus 40-90%  
719 reported for temperate regions could be related to the shallow habitat sampled in our surveys (<2 m  
720 depth low tide). The calcifying macroalgae genera *Amphiroa* and *Jania* using  $\text{HCO}_3^-$  and diffusive  
721  $\text{CO}_2$  influenced by the calcification process (strategy 4) were present in the macroalgal communities  
722 along the GC and high  $\delta^{13}\text{C}$  values (similar to strategy 1). Because the ongoing ocean acidification,  
723 these calcifying organisms constitute excellent ecological sentinels in the GC.



724 Finally, diverse authors have reported significant correlations between  $\delta^{13}\text{C}$  signal and latitude,  
725 mainly related to the light and temperature. However, in the latitude range (21°-31°N) in our study,  
726 the linear regression analyzes showed a low correlation for the  $\delta^{13}\text{C}$ -macroalgal dataset classified by  
727 morphofunctional groups and genus, being negative for Rhodophyta and Ochrophyta and positive  
728 for Chlorophyta. Because the shallow habitats occupied by macroalgal communities in the GC were  
729 high-light environments with narrow ranges in temperature, not clear patterns along the GC latitudes.  
730 However, detectable changes were observed in the  $\delta^{13}\text{C}$ -macroalgal and the proportion of specimens  
731 with different carbon uptake strategies among coastal sectors. For example, the facultative uptake of  
732  $\text{HCO}_3^-$  and  $\text{CO}_2$  was dominant in the macroalgal shallow communities in the GC (60 to 90% of  
733 specimens), but in the coastal sector P1 was the specialized strategy of only  $\text{HCO}_3^-$  use the dominant  
734 strategy (68%), and significant at C1 (37%).

735 Our research is the first approximation to understand the  $\delta^{13}\text{C}$ -macroalgal variability in one of the  
736 most diverse marine ecosystems in the world, the Gulf of California. We did not pretend to resolve  
737 the intricate processes controlling the variations of  $\delta^{13}\text{C}$  or  $\Delta^{13}\text{C}$ -macroalgal during carbon  
738 assimilation and respiration and determine the isolated influence of each environmental factor.  
739 Controlled experiments in laboratory and mesocosm type in combination with field studies are  
740 required to elucidate the complex processes controlling the  $\delta^{13}\text{C}$ -macroalgal. Even so, the  $\delta^{13}\text{C}$ -  
741 macroalgal was a good proxy to identify  $\text{CO}_2$  or  $\text{HCO}_3^-$  source in photosynthesis and to infer the  
742 presence or absence of CCM's and identify the macroalgae lineages that could be in competitive  
743 advantage based on their carbon uptake strategy and identify their geographical distribution along  
744 GC.

745 Under the current conditions of climate change and their effects as ocean acidification in progress  
746 and the bloom-forming macroalgae events that increases in México and worldwide, the analysis of

747  $\delta^{13}\text{C}$ -macroalgal constitute an excellent tool to help to predict the prevalence and shift of species in  
748 a macroalgal communities' focused on carbon metabolism.

## 749 **6. Data Availability Statement**

750 Data set are each permanently deposited Soto-Jimenez, MARTIN F; Velázquez-Ochoa, Roberto;  
751 Ochoa Izaguirre, Maria Julia. Earth and Space Science Open Archive ESSOAr; Washington, Nov  
752 25, 2020. DOI:10.1002/essoar.10504972.1

753 [https://search.proquest.com/openview/2060de58b217ca47495469b53ae2f347/1?pq-](https://search.proquest.com/openview/2060de58b217ca47495469b53ae2f347/1?pq-origsite=gscholar&cbl=4882998)

754 [origsite=gscholar&cbl=4882998](https://search.proquest.com/openview/2060de58b217ca47495469b53ae2f347/1?pq-origsite=gscholar&cbl=4882998)

## 755 **7. Author contribution**

756 Velázquez-Ochoa R. participate in the collection, processing, and analysis of the samples as a part  
757 of his master's degree thesis. Ochoa-Izaguirre J. also participate in sample collections and  
758 identified macroalgae specimens. Soto-Jiménez M.F. coordinated the research, was the thesis  
759 director, and prepared the manuscript with contributions from all co-authors.

## 760 **8. Competing interests**

761 The authors declare that they have no conflict of interest.

## 762 **9. Acknowledgements**

763 The authors would like to thank H. Bojórquez-Leyva, Y. Montaña-Ley, and A. Cruz-López for  
764 their invaluable assistance with field and laboratory work. Thanks to S. Soto Morales for the  
765 English revision. UNAM-PAPIIT IN206409 and IN208613 provided financial support and  
766 UNAM-PASPA supported to MF Soto-Jimenez for Sabbatical year.

767 **10. References**

- 768 Abbot, I. A., and Hollenberg, G.: Marine algae of California. Standford University Press, California.  
769 1976.
- 770 Aguilar-Rosas, L. E., and R. Aguilar-Rosas, R.: Ficogeografía de las algas pardas (Phaeophyta) de  
771 la península de Baja California, in: Biodiversidad Marina y Costera de México (Comisión Nacional  
772 Biodiversidad y CIQRO, México), edited by: Salazar-Vallejo, S. I. and González, N. E., 197-206,  
773 1993.
- 774 Aguilar-Rosas, L. E., Pedroche, F. F., and Zertuche-González, J. A.: Algas Marinas no nativas en la  
775 costa del Pacífico Mexicano. Especies acuáticas invasoras en México. Comisión Nacional para el  
776 Conocimiento y Uso de la Biodiversidad, México, 211-222, 2014.
- 777 Álvarez-Borrego, S.: Gulf of California., in: Ecosystems of the World, 26. *Estuaries and Enclosed*  
778 *Seas*, (Elsevier, Amsterdam), Edited by: Ketchum BH., 427–449, 1983.
- 779 Anthony, K. R., Ridd, P. V., Orpin, A. R., Larcombe, P., and Lough, J.: Temporal variation of light  
780 availability in coastal benthic habitats: Effects of clouds, turbidity, and tides, *Limnol. Oceanogr.*,  
781 49(6), 2201-2211, <https://doi.org/10.4319/lo.2004.49.6.2201>, 2004.
- 782 Axelsson, L., Larsson, C., and Ryberg, H.: Affinity, capacity and oxygen sensitivity of two different  
783 mechanisms for bicarbonate utilization in *Ulva lactuca* L. (Chlorophyta), *Plant Cell Environ.*, 22,  
784 969–978, <https://doi.org/10.1046/j.1365-3040.1999.00470.x>, 1999.
- 785 Balata, D., Piazzzi, L., and Rindi, F.: Testing a new classification of morphological functional groups  
786 of marine macroalgae for the detection of responses to stress, *Mar. Biol.*, 158, 2459–2469,  
787 <https://doi.org/10.1007/s00227-011-1747-y>, 2011.
- 788 Bastidas-Salamanca, M., Gonzalez-Silvera, A., Millán-Núñez, R., Santamaria-del-Angel, E., and  
789 Frouin, R.: Bio-optical characteristics of the Northern Gulf of California during June 2008, *Int. J.*  
790 *Oceanogra.*, <https://doi.org/10.1155/2014/384618>, 2014.
- 791 Bauwe, H., Hagemann, M., and Fernie, A. R.: Photorespiration: players, partners and origin, *Trends*  
792 *Plant Sci.*, 15(6), 330–336, <https://doi.org/10.1016/j.tplants.2010.03.006>, 2010.

- 793 Beardall, J., and Giordano, M.: Ecological implications of microalgal and cyanobacterial CO<sub>2</sub>  
794 concentrating mechanisms, and their regulation, *Funct. Plant Biol.*, 29(3), 335–347,  
795 <https://doi.org/10.1071/PP01195>, 2002.
- 796 Bold, C. H., and Wynne, J. M.: Introduction to the Algae: Structure and reproduction. Prentice-Hall,  
797 Incorporated, 1978.
- 798 Bowes, G. W.: Carbonic anhydrase in marine algae, *Plant Physiol.*, 44:726–732,  
799 <https://doi.org/10.1104/pp.44.5.726>, 1969.
- 800 Bray, N. A.: Thermohaline circulation in the Gulf of California, *J. Geophys. Res. Oceans.*, 93(C5),  
801 4993–5020, <https://doi.org/10.1029/JC093iC05p04993>, 1988.
- 802 Brodeur, J. R., Chen, B., Su, J., Xu, Y. Y., Hussain, N., Scaboo, K. M., Zhang, Y., Testa, J. M. and  
803 Cai, W. J.: Chesapeake Bay inorganic carbon: Spatial distribution and seasonal variability, *Front.*  
804 *Mar. Sci.*, <https://doi.org/10.3389/fmars.2019.000996>, 99, 2019.
- 805 Brusca, R. C., Findley, L. T., Hastings, P. A., Hendrickx, M. E., Cosio, J. T., and van der Heiden, A.  
806 M.: Macrofaunal diversity in the Gulf of California. Biodiversity, ecosystems, and conservation in  
807 Northern Mexico, 179, 2005.
- 808 Burnham, K. P., and Anderson, D. R.: A practical information-theoretic approach, Model selection  
809 and multimodel inference, 2nd ed. Springer, New York, 2. 2002.
- 810 Carrillo, L., and Palacios-Hernández, E.: Seasonal evolution of the geostrophic circulation in the  
811 northern Gulf of California, *Estuar. Coast. Shelf Sci.*, 54(2), 157–173,  
812 <https://doi.org/10.1006/ecss.2001.0845>, 2002.
- 813 Carvalho, M. C. and Eyre, B. D.: Carbon stable isotope discrimination during respiration in three  
814 seaweed species, *Mar. Ecol. Prog. Ser.*, 437:41–49. <https://doi.org/10.3354/meps09300>, 2011.
- 815 Carvalho, M. C., Hayashizaki, K., Ogawa, H., and Kado, R.: Preliminary evidence of growth  
816 influence on carbon stable isotope composition of *Undaria pinnatifida*, *Mar. Res. Indones.*, 32, 185-  
817 188, 2007.
- 818 Carvalho, M. C., Hayashizaki, K., and Ogawa, H.: Effect of pH on the carbon stable isotope

819 fractionation in photosynthesis by the kelp *Undaria pinnatifida*, *Coast. Mar. Sci.*, 34(1), 135-139,  
820 2010a.

821 Carvalho, M. C., Hayashizaki, K. I., and Ogawa, H.: Temperature effect on carbon isotopic  
822 discrimination by *Undaria pinnatifida* (Phaeophyta) in a closed experimental system<sup>1</sup>, *J. Phycol.*,  
823 46(6), 1180-1186, <https://doi.org/10.1111/j.1529-8817.2010.00895.x>, 2010b.

824 Cerling, T. E., Wang, Y., and Quade, J.: Expansion of C4 ecosystems as an indicator of global  
825 ecological change in the late Miocene, *Nature*, 361 (6410), 344–345,  
826 <https://doi.org/10.1038/361344a0>, 1993.

827 Comeau, S., Carpenter, R. C., and Edmunds, P. J.: Coral reef calcifiers buffer their response to ocean  
828 acidification using both bicarbonate and carbonate, *Proc. Bio. Sci.*, 280(1753), 20122374,  
829 <https://doi.org/10.1098/rspb.2012.2374>, 2012.

830 CNA (Comisión Nacional del Agua): Atlas del agua en México, 2012.

831 Cornelisen, C. D., Wing, S. R., Clark, K. L., Hamish Bowman, M., Frew, R. D., and Hurd, C. L.:  
832 Patterns in the  $\delta^{13}\text{C}$  and  $\delta^{15}\text{N}$  signature of *Ulva pertusa*: interaction between physical gradients and  
833 nutrient source pools, *Limnol. Oceanogr.*, 52(2), 820-832, 2007.

834 Cornwall, C. E., Revill, A. T., and Hurd, C. L.: High prevalence of diffusive uptake of  $\text{CO}_2$  by  
835 macroalgae in a temperate subtidal ecosystem, *Photosynth. Res.*, 124, 181–190,  
836 <https://doi.org/10.1007/s11120-015-0114-0>, 2015.

837 Dawson, E. Y.: The marine algae of the Gulf of California, *Allan Hancock Pac. Exped.*, 3(10), [i-  
838 v+] 189–453, 1944.

839 Dawson, E. Y.: Marine red algae of Pacific México. Part 2. *Cryptonemiales* (cont.), *Allan Hancock*  
840 *Pac. Exped.*, 17(2), 241–397, 1954.

841 Dawson, E. Y.: How to know the seaweeds, Dubuque, Iowa, USA. W.M.C. Brown. Co. Publishers.  
842 pp 197., 1956.

843 Dawson, E. Y.: The marine red algae of Pacific Mexico, Part 4, Gigartinales. *Allan Hancock Pacific*  
844 *Exped.*, 2, 191-343, 1961.

- 845 Dawson, E. Y.: Marine red algae of Pacific México. Part 7. *Ceramiales*: Ceramiaceae,  
846 Delesseriaceae, Allan Hancock Pac. Exped., 26(1), 1–207, 1962.
- 847 Dawson, E. Y.: Marine red algae of Pacific México. Part 8. *Ceramiales*: Dasyaceae, Rhodomelaceae.  
848 Nova Hedwigia, 6, 437–476, 1963.
- 849 Díaz-Pulido, G., Cornwall, C., Gartrell, P., Hurd, C., and Tran, D. V.: Strategies of dissolved  
850 inorganic carbon use in macroalgae across a gradient of terrestrial influence: implications for the  
851 Great Barrier Reef in the context of ocean acidification, Coral Reefs, 35(4), 1327-1341,  
852 <https://doi.org/10.1007/s00338-016-1481-5> 2016.
- 853 Doubnerová, V., and Ryšlavá, H.: What can enzymes of C4 photosynthesis do for C3 plants under  
854 stress?, *Plant Sci.*, 180(4), 575–583, <https://doi.org/10.1016/j.plantsci.2010.12.005>, 2011.
- 855 Draper, N. R., and Smith, H.: Applied regression analysis, edited by: John Wiley & Sons (Vol. 326),  
856 1998.
- 857 Drechsler, Z., and Beer, S.: Utilization of inorganic carbon by *Ulva lactuca*. *Plant Physiol.*, 97,  
858 1439–1444, <https://doi.org/10.1104/pp.97.4.1439>, 1991.
- 859 Drechsler, Z., Sharkia, R., Cabantchik, Z. I., and Beer, S. Bicarbonate uptake in the marine  
860 macroalga *Ulva* sp. is inhibited by classical probes of anion exchange by red blood cells, *Planta*,  
861 191(1), 34–40, <https://doi.org/10.1007/BF00240893>, 1993.
- 862 Dreckmann, K. M.: El género *Gracilaria* (Gracilariaceae, Rhodophyta) en el Pacífico centro-sur  
863 mexicano, Monografías ficológicas, 1, 77-118, 2002.
- 864 Dudgeon, S. R., Davison, I. R., and Vadas, R. L. Freezing tolerance in the intertidal red algae  
865 *Chondrus crispus* and *Mastocarpus stellatus*: Relative importance of acclimation and adaptation,  
866 *Mar Biol.*, 106(3), 427–436, <https://doi.org/10.1007/BF01344323>, 1990.
- 867 Dudley, B. D., Barr, N. G., and Shima, J. S.: Influence of light intensity and nutrient source on  $\delta^{13}\text{C}$   
868 and  $\delta^{15}\text{N}$  signatures in *Ulva pertusa*, *Aquat. Biol.*, 9(1), 85–93, <https://doi.org/10.3354/AB00241>,  
869 2010.
- 870 Ehleringer, J. R., Sage, R. F., Flanagan, L. B., and Pearcy, R. W.: Climate change and the evolution

871 of C4 photosynthesis, *Trends Ecol. Evol.*, 6(3), 95–99, <https://doi.org/10.1073/pnas.1718988115>,  
872 1991.

873 Enríquez, S., and Rodríguez-Román, A.: Effect of water flow on the photosynthesis of three marine  
874 macrophytes from a fringing-reef lagoon, *Mar. Ecol. Prog. Ser.*, 323, 119–132,  
875 <https://doi.org/10.3354/meps323119>, 2006.

876 Espinoza-Avalos, J.: Macroalgas marinas del Golfo de California, *Biodiversidad marina y costera*  
877 *de México (CONABIO- CIQRO, México)*, edited by: Salazar-Vallejo, S.I., González, N. E., 328–  
878 357, 1993.

879 Espinosa-Carreón, T. L., and Valdez-Holguín, E.: Variabilidad interanual de clorofila en el Golfo de  
880 California. *Ecol. Apl.*, 6(1-2), 83–92, 2007.

881 Espinosa-Carreón, T. L., and Escobedo-Urías, D.: South region of the Gulf of California large marine  
882 ecosystem upwelling, fluxes of CO<sub>2</sub> and nutrients, *Environ Dev.*, 22, 42–51,  
883 <https://doi.org/10.1016/j.envdev.2017.03.005>, 2017.

884 Gateau, H., Solymosi, K., Marchand, J., and Schoefs, B.: Carotenoids of microalgae used in food  
885 industry and medicine. *Mini-Rev. Med. Chem.*, 17(13), 1140–1172,  
886 <https://doi.org/10.2174/1389557516666160808123841>, 2017.

887 Gilbert, J. Y., and Allen, W. E.: The phytoplankton of the Gulf of California obtained by the “E.W.  
888 Scripps” in 1939 and 1940, *J. Mar. Res.*, 5, 89–110, [https://doi.org/10.1016/0022-0981\(67\)90008-](https://doi.org/10.1016/0022-0981(67)90008-1)  
889 1, 1943.

890 Giordano, M., Beardall, J., and Raven, J. A.: CO<sub>2</sub> concentrating mechanisms in algae: mechanisms,  
891 environmental modulation and evolution, *Annu. Rev. Plant Biol.*, 66:99–131,  
892 <https://doi.org/10.1146/annurev.arplant.56.032604.144052>, 2005.

893 Gowik, U., and Westhoff, P.: The path from C3 to C4 photosynthesis, *Plant Physiol.*, 155(1), 56–63,  
894 <https://doi.org/10.1104/pp.110.165308>, 2012.

895 Hepburn, C. D., Pritchard, D. W., Cornwall, C. E., McLeod, R. J., Beardall, J., Raven, J. A., and  
896 Hurd, C. L.: Diversity of carbon use strategies in a kelp forest community: implications for a high  
897 CO<sub>2</sub> ocean, *Glob. Change Biol.*, 17, 2488–2497. <https://doi.org/10.1111/j.1365-2486.2011.02411.x>,

898 2011.

899 Hinger, E. N., Santos, G. M., Druffel, E. R. M., and Griffin, S.: Carbon isotope measurements of  
900 surface seawater from a time-series site off Southern California, *Radiocarbon* 52(1):69–89, 2010.

901 Hofmann, L., and Heesch, S.: Latitudinal trends in stable isotope signatures and carbon-  
902 concentrating mechanisms of northeast Atlantic rhodoliths, *Biogeosciences*, 15, 6139–6149,  
903 <https://doi.org/10.5194/bg-15-6139-2018>, 2018.

904 Hopkinson, B. M., Dupont, C. L., Allen, A. E., and Morel, F. M. M.: Efficiency of the CO<sub>2</sub>-  
905 concentrating mechanism of diatoms, *Proc. Natl. Acad. Sci. U.S.A.*, 108, 3830–3837,  
906 <https://doi.org/10.1073/pnas.1018062108>, 2011.

907 Hopkinson, B. M., Young, J. N., Tansik, A. L., and Binder, B. J.: The minimal CO<sub>2</sub> concentrating  
908 mechanism of *Prochlorococcus* MED4 is effective and efficient, *Plant Physiol.*, 166, 2205–2217,  
909 <https://doi.org/10.1104/pp.114.247049>, 2014.

910 Hu, X., Burdige, D. J., and Zimmerman, R. C.:  $\delta^{13}\text{C}$  is a signature of light availability and  
911 photosynthesis in seagrass, *Limnol. Oceanogr.*, 57(2), 441–448,  
912 <https://doi.org/10.4319/lo.2012.57.2.0441>, 2012.

913 Hurd, C. L.: Water motion, marine macroalgal physiology and production, *J. Phycol.*, 36, 453–472,  
914 <https://doi.org/10.1046/j.1529-8817.2000.99139.x>, 2000.

915 Iluz, D., Fermani, S., Ramot, M., Reggi, M., Caroselli, E., Prada, F., Dubinsky, Z., Goffredo, S. and  
916 Falin, G.: Calcifying response and recovery potential of the brown alga *Padina pavonica* under ocean  
917 acidification, *ACS Earth Space Chem.*, 1(6), 316–323,  
918 <https://doi.org/10.1021/acsearthspacechem.7b00051>, 2017.

919 Iñiguez, C., Galmés, J., and Gordillo, F. J.: Rubisco carboxylation kinetics and inorganic carbon  
920 utilization in polar versus cold-temperate seaweeds, *J. Exp. Bot.*, 70(4), 1283–1297.  
921 <https://doi.org/10.1093/jxb/ery443>, 2019.

922 Jensen, E. L., Maberly, S. C., and Gontero, B.: Insights on the functions and ecophysiological  
923 relevance of the diverse carbonic anhydrases in microalgae, *Int. J. Mol. Sci.*, 21(8), 2922,  
924 <https://doi.org/10.3390/ijms21082922>, 2020.



925 Johansson, G., and Snoeijs, P.: Macroalgal photosynthetic responses to light in relation to thallus  
926 morphology and depth zonation, *Mar. Ecol. Prog. Ser.*, 244, 63-72, <https://doi:10.3354/meps244063>,  
927 2002.

928 Kim, M. S., Lee, S. M., Kim, H. J., Lee, S. Y., Yoon, S. H., and Shin, K. H.: Carbon stable isotope  
929 ratios of new leaves of *Zostera marina* in the mid-latitude region: implications of seasonal variation  
930 in productivity, *J. Exp. Mar Biol. Ecol.*, 461, 286–296, <https://doi.org/10.1016/j.jembe.2014.08.015>,  
931 2014.

932 Klenell, M., Snoeijs, P., and Pedersen, M.: Active carbon uptake in *Laminaria digitata* and *L.*  
933 *saccharina* (Phaeophyta) is driven by a proton pump in the plasma membrane, *Hydrobiologia*, 514,  
934 41–53, <https://doi.org/10.1023/B:hydr.0000018205.80186.3e>, 2004.

935 Kübler, J. E., and Davison, I. R.: High-temperature tolerance of photosynthesis in the red alga  
936 *Chondrus crispus*, *Mar. Biol.*, 117(2), 327–335. <https://doi.org/10.1007/BF00345678>, 1993.

937 Kübler, J. E., and Dudgeon, S. R.: Predicting effects of ocean acidification and warming on algae  
938 lacking carbon concentrating mechanisms, *PLoS One*, 10 (7),  
939 <https://doi.org/10.1371/journal.pone.0132806>, 2015.

940 Lapointe, B. E., and Duke, C. S.: Biochemical strategies for growth of *Gracilaria tikvahiae*  
941 (Rhodophyta) in relation to light intensity and nitrogen availability, *J. Phycol.*, 20(4), 488–495.  
942 <https://doi.org/10.1111/j.0022-3646.1984.00488.x>, 1984.

943 Littler, M. M., and Littler, D. S.: The evolution of thallus form and survival strategies in benthic  
944 marine macroalgae: field and laboratory tests of a functional form model, *Am Nat.*, 116, 25–44,  
945 1980.

946 Littler, M. M., and Arnold, K. E.: Primary productivity of marine macroalgal functional-form groups  
947 from south-western North America, *J. Phycol.*, 18, 307–311, [https://doi.org/10.1111/j.1529-](https://doi.org/10.1111/j.1529-8817.1982.tb03188.x)  
948 [8817.1982.tb03188.x](https://doi.org/10.1111/j.1529-8817.1982.tb03188.x), 1982.

949 Lobban, C. S., Harrison, P. J., and Harrison, P. J.: Seaweed ecology and physiology. Cambridge  
950 University Press, 1994.

951 Lovelock, C. E., Reef, R., Raven, J. A., and Pandolfi, J. M.: Regional variation in  $\delta^{13}\text{C}$  of coral reef  
952 macroalgae, *Limnol. Oceanogr.*, <https://doi.org/10.1002/lno.11453>, 2020.

953 Lluch-Cota, S. E., Aragon-Noriega, E. A., Arreguin-Sanchez, F., Aurioles-Gamboa, D., Bautista-  
954 Romero, J. J., Brusca, R. C., Cervantes-Duarte, R., Cortes-Altamirano, R., Del-MonteLuna, P.,  
955 Esquivel-Herrera, A., Fernández, G., Hendrickx, M. E., Hernandez-Vazquez, S., Herrera-Cervantes,  
956 H., Kahru, M., Lavin, M., Lluch-Belda, D., Lluch-Cota, D. B., Lopez-Martinez, J., Marinone, S. G.,  
957 Nevarez-Martinez, M. O., Ortega-Garcia, S., Palacios-Castro, E., Pares-Sierra, A., Ponce-Diaz, G.,  
958 RamirezRodriguez, M., Salinas-Zavala, C. A., Schwartzlose, R. A., and Sierra-Beltran, A. P.: The  
959 Gulf of California: Review of ecosystem status and sustainability challenges, *Prog. Oceanogr.*, 73,  
960 1–26, 2007.

961 Maberly, S. C., Raven, J. A. and Johnston, A. M.: Discrimination between  $^{12}\text{C}$  and  $^{13}\text{C}$  by marine  
962 plants, *Oecologia*, 91,481–492, <https://doi.org/10.1007/BF00650320>, 1992.

963 Mackey, A. P., Hyndes, G. A., Carvalho, M. C., and Eyre, B. D.: Physical and biogeochemical  
964 correlates of spatio-temporal variation in the  $\delta^{13}\text{C}$  of marine macroalgae, *Estuar. Coast. Shelf Sci.*,  
965 157, 7-18, <https://doi.org/10.1016/j.ecss.2014.12.040>, 2015.

966 Madsen, T. V., and Maberly, S. C.: High internal resistance to  $\text{CO}_2$  uptake by submerged  
967 macrophytes that use  $\text{HCO}_3^-$ : measurements in air, nitrogen and helium, *Photosynth. Res.*, 77(2-3),  
968 183–190, <https://doi.org/10.1023/A:1025813515956>, 2003.

969 Marinone, S. G., and Lavín, M. F.: Residual flow and mixing in the large islands’ region of the  
970 central Gulf of California: Nonlinear processes in geophysical fluid dynamics, Springer, Dordrechm,  
971 [http://doi-org-443.webvpn.fjmu.edu.cn/10.1007/978-94-010-0074-1\\_13](http://doi-org-443.webvpn.fjmu.edu.cn/10.1007/978-94-010-0074-1_13), 2003.

972 Marinone, S. G.: A note on “Why does the Ballenas Channel have the coldest SST in the Gulf of  
973 California?”. *Geophysical research letters*, 34(2). <https://doi.org/10.1029/2006GL028589>, 2007.

974 Marconi, M., Giordano, M., and Raven, J. A.: Impact of taxonomy, geography and depth on the  $\delta^{13}\text{C}$   
975 and  $\delta^{15}\text{N}$  variation in a large collection of macroalgae, *J. Phycol.*, 47, 1023–1035,  
976 <https://doi.org/10.1111/j.1529-8817.2011.01045.x>, 2011.

977 Martínez-Díaz-de-León, A.: Upper-ocean circulation patterns in the Northern Gulf of California,  
978 expressed in Ers-2 synthetic aperture radar imagery, *Cienc. Mar.*, 27(2), 209–221,  
979 <https://doi.org/10.7773/cm.v27i2.465>, 2001.

- 980 Martínez-Díaz-de-León, A., Pacheco-Ruíz, I., Delgadillo-Hinojosa, F., Zertuche-González, J. A.,  
981 Chee-Barragán, A., Blanco-Betancourt, R., Guzmán-Calderón, J. M., and Gálvez-Telles, A.: Spatial  
982 and temporal variability of the sea surface temperature in the Ballenas-Salsipuedes Channel (central  
983 Gulf of California), *J. Geophys. Res. Oceans*, 111(C2), <https://doi.org/10.1029/2005JC002940>,  
984 2006.
- 985 Masojidek, J., Kopecká, J., Koblížek, M., and Torzillo, G.: The xanthophyll cycle in green algae  
986 (Chlorophyta): its role in the photosynthetic apparatus, *Plant Biol.*, 6(3), 342–349,  
987 <https://doi.org/10.1055/s-2004-820884>, 2004.
- 988 McConnaughey, T. A., Burdett, J., Whelan, J. F., and Paull, C. K.: Carbon isotopes in biological  
989 carbonates: respiration and photosynthesis, *Geochim. Cosmochim. Ac.*, 61(3), 611–622,  
990 [https://doi.org/10.1016/S0016-7037\(96\)00361-4](https://doi.org/10.1016/S0016-7037(96)00361-4), 1997.
- 991 Mercado, J. M., De los Santos, C. B., Pérez-Lloréns, J. L., and Vergara, J. J.: Carbon isotopic  
992 fractionation in macroalgae from Cadiz Bay (Southern Spain): comparison with other bio-  
993 geographic regions, *Estuar, Coast. Shelf Sci.*, 85, 449–458,  
994 <https://doi.org/10.1016/j.ecss.2009.09.005>, 2009.
- 995 Murru, M., and Sandgren, C.D.: Habitat matters for inorganic carbon acquisition in 38 species of red  
996 macroalgae (Rhodophyta) from Puget Sound, Washington, USA. *J. Phycol.*, 40, 837–845.  
997 <https://doi.org/10.1111/j.1529-8817.2004.03182.x>, 2004.
- 998 Nielsen, S. L., and Jensen, K. S.: Allometric settling of maximal photosynthetic growth rate to  
999 surface/volume ratio, *Limnol. Oceanogr.*, 35(1), 177–180,  
1000 <https://doi.org/10.4319/lo.1990.35.1.0177>, 1990.
- 1001 Norris, J. N.: The marine algae of the northern Gulf of California, Ph. D. dissertation, University of  
1002 California, Santa Barbara, 575 pp., 1975.
- 1003 Norris, J. N.: Studies on *Gracilaria Grev.*(Gracilariaceae, Rhodophyta) from the Gulf of California,  
1004 Mexico. *Taxonomy of Economic Seaweeds*, California Sea Grant College Program, California, I,  
1005 123-135, 1985.
- 1006 Norris, J. N.: Marine algae of the northern Gulf of California: Chlorophyta and Phaeophyceae,

1007 Smithsonian contr. Bot., no. 94, <https://doi.org/10.5479/si.19382812.96>, 2010.

1008 Oehlert, A. M., Lamb-Wozniak, K. A., Devlin, Q. B., Mackenzie, G. J., Reijmer, J. J., and Swart, P.  
1009 K.: The stable carbon isotopic composition of organic material in platform derived sediments:  
1010 implications for reconstructing the global carbon cycle, *Sedimentology*, 59(1), 319–335,  
1011 <https://doi.org/10.1111/j.1365-3091.2011.01273.x>, 2012.

1012 Ochoa-Izaguirre, M. J., Aguilar-Rosas, R., and Aguilar-Rosas, L. E.: Catálogo de Macroalgas de las  
1013 lagunas costeras de Sinaloa, Serie Lagunas Costeras, Edited by Páez-Osuna, F., UNAM, ICMYL,  
1014 México, pp 117, 2007.

1015 Ochoa-Izaguirre, M. J., and Soto-Jiménez, M. F.: Variability in nitrogen stable isotope ratios of  
1016 macroalgae: consequences for the identification of nitrogen sources, *J. Phycol.*, 51, 46–65,  
1017 <https://doi.org/10.1111/jpy.12250>, 2015.

1018 Páez-Osuna, F., Piñón-Gimate, A., Ochoa-Izaguirre, M. J., Ruiz-Fernández, A. C., Ramírez-  
1019 Reséndiz, G., and Alonso-Rodríguez, R.: Dominance patterns in macroalgal and phytoplankton  
1020 biomass under different nutrient loads in subtropical coastal lagoons of the SE Gulf of California,  
1021 *Mar. Pollut. Bull.*, 77(1-2), 274-281, <https://doi.org/10.1016/j.marpolbul.2013.09.048>, 2013.

1022 Páez-Osuna, F., Álvarez-Borrego, S., Ruiz-Fernández, A. C., García-Hernández, J., Jara-Marini, E.,  
1023 Bergés-Tiznado, M. E., Piñón-Gimate, A., Alonso-Rodríguez, R., Soto-Jiménez, M. F., Frías-  
1024 Espericueta, M. G., Ruelas-Inzunza, J. R., Green-Ruíz, C. R., Osuna-Martínez, C. C., and Sánchez-  
1025 Cabeza, J. A.: Environmental status of the Gulf of California: a pollution review, *Earth-Sci. Rev.*,  
1026 166, 181–205, <https://doi.org/10.1016/j.earscirev.2016.09.015>, 2017.

1027 Pedroche, F. F., and Senties, A.: Ficología marina mexicana: Diversidad y Problemática actual,  
1028 *Hidrobiológica*, 13(1), 23–32, 2003.

1029 Rautenberger, R., Fernández, P. A., Strittmatter, M., Heesch, S., Cornwall, C. E., Hurd, C. L., and  
1030 Roleda, M. Y.: Saturating light and not increased carbon dioxide under ocean acidification drive  
1031 photosynthesis and growth in *Ulva rigida* (Chlorophyta), *Ecol. Evol.*, 5(4), 874–888,  
1032 <https://doi.org/10.1002/ece3.1382>, 2015.

1033 Raven, J. A., Johnston, A. M., Kübler, J. E., Korb, R. E., McInroy, S. G., Handley, L. L., Scrimgeour,  
1034 C. M., Walker, D. I., Beardall, J., Clayton, M. N., Vanderklift, M., Fredriksen, S., and Dunton, K.  
1035 H.: Seaweeds in cold seas: evolution and carbon acquisition, *Ann. Bot.*, 90, 525–536.  
1036 <https://doi.org/10.1093/aob/mcf171>, 2002a.

- 1037 Raven, J. A., Johnshon, A. M., Kübler, J. E., Korb, R. E., McInroy, S. G., Handley, L. L.,  
1038 Scrimgeour, C. M., Walker, D. I., Beardall, J., Vanderklift, M., Fredriksen, S., and Dunton, K. H.:  
1039 Mechanistic interpretation of carbon isotope discrimination by marine macroalgae and seagrasses,  
1040 *Funct. Plant Biol.*, 29:355–378, <https://doi.org/10.1071/PP01201>, 2002b.
- 1041 Raven, J. A., Ball, L. A., Beardall, J., Giordano, M., and Maberly, S. C.: Algae lacking carbon-  
1042 concentrating mechanisms, *Can. J. Bot.*, 83(7), 879–890, <https://doi.org/10.1139/b05-074>, 2005.
- 1043 Raven, J. A., and Beardall, J.: The ins and outs of CO<sub>2</sub>, *J. Exp. Bot.*, 67(1), 1–13,  
1044 <https://doi.org/10.1093/jxb/erv451>, 2016.
- 1045 Roberts, K., Granum, E., Leegood, R. C., and Raven, J. A.: C<sub>3</sub> and C<sub>4</sub> pathways of photosynthetic  
1046 carbon assimilation in marine diatoms are under genetic, not environmental control, *Plant Physiol.*,  
1047 145(1), 230–235, <https://doi.org/10.1104/pp.107.102616>, 2007.
- 1048 Roden, G. I.: Oceanographic and meteorological aspects of the Gulf of California, 1958.
- 1049 Roden, G. I., and Groves, G. W.: Recent oceanographic investigations in the Gulf of California, *J.*  
1050 *Mar. Res.*, 18(1), 10–35, 1959.
- 1051 Roden, G. I., and Emilsson, L.: Physical oceanography of the Gulf of California. Symposium Golfo  
1052 de California, Universidad Nacional Autónoma de México, Mazatlán, Sinaloa, México, 1979.
- 1053 Rusnak, G. A., Fisher, R. L., and Shepard, F. P.: Bathymetry and faults of Gulf of California. In: van  
1054 Andel, Tj. H. and G.G. Shor, Jr. (editors), *Marine Geology of the Gulf of California: A symposium,*  
1055 *AAPG Memoir*, 3, 59–75, <https://doi.org/10.1306/M3359C3>, 1964.
- 1056 Sand-Jensen, K., and Gordon, D.: Differential ability of marine and freshwater macrophytes to utilize  
1057 HCO<sub>3</sub><sup>-</sup> and CO<sub>2</sub>, *Mar. Biol.*, 80, 247–253, <https://doi.org/10.1111/j.1469-8137.1981.tb03198.x>,  
1058 1984.
- 1059 Sanford, L. P., and Crawford, S. M.: Mass transfer versus kinetic control of uptake across solid-  
1060 water boundaries, *Limnol. Oceanogr.*, 45, 1180–1186, <https://doi.org/10.4319/lo.2000.45.5.1180>,  
1061 2000.

1062 Santamaría-del-Angel, E., Alvarez-Borrego, S., and Müller-Karger, F. E.: Gulf of California  
1063 biogeographic regions based on coastal zone color scanner imagery, *J. Geophys. Res.*, 99,  
1064 7411–7421, <https://doi.org/10.1029/93JC02154>, 1994.

1065 Santos, G. M., Ferguson, J., Acaylar, K., Johnson, K. R., Griffin, S., and Druffel, E.:  $\Delta^{14}\text{C}$  and  $\delta^{13}\text{C}$   
1066 of seawater DIC as tracers of coastal upwelling: A 5-year time series from Southern California,  
1067 *Radiocarbon*, 53(4), 669–677, <https://doi.org/10.1017/S0033822200039126>, 2011.

1068 Setchell, W., and Gardner, N.: The marine algae of the Pacific Coast of North America. Part II  
1069 Chlorophyceae, *Univ. Calif. Publ. Bot.*, 8, 139–374, <https://doi.org/10.5962/bhl.title.5719>, 1920.

1070 Setchell, W., and Gardner, N.: The marine algae: Expedition of the California Academy of Sciences  
1071 to the Gulf of California in 1921, *Proc. Calif. Acad. Sci.*, 4th series, 12(29), 695–949, 1924.

1072 Sharkey, T. D., and Berry, J. A.: Carbon isotope fractionation of algae as influenced by an inducible  
1073  $\text{CO}_2$  concentrating mechanism. *Inorganic carbon uptake by aquatic photosynthetic organisms*, 1985.

1074 Stepien, C. C.: Impacts of geography, taxonomy and functional group on inorganic carbon use  
1075 patterns in marine macrophytes, *J. Ecol.*, 103(6), 1372–1383, [https://doi.org/10.1111/1365-](https://doi.org/10.1111/1365-2745.12451)  
1076 [2745.12451](https://doi.org/10.1111/1365-2745.12451), 2015.

1077 Teichberg, M., Fox, S. E., Olsen, Y. S., Valiela, I., Martinetto, P., Iribarne, O., Muto, E. Y., Petti,  
1078 M. A., Cobrisier, T. N., Soto-Jiménez, M., Páez-Osuna, F., Castro, P., Freitas, H., Zitelli, A.,  
1079 Cardinaletti, M. and Tagliapietra, D.: Eutrophication and macroalgal blooms in temperate and  
1080 tropical coastal waters: nutrient enrichment experiments with *Ulva* spp., *Global Change Biology*,  
1081 16(9), 2624–2637, <https://doi.org/10.1111/j.1365-2486.2009.02108.x>, 2010.

1082 Valiela, I., Liu, D., Lloret, J., Chenoweth, K., and Hanacek, D.: Stable isotopic evidence of  
1083 nitrogen sources and  $\text{C}_4$  metabolism driving the world’s largest macroalgal green tides in the  
1084 Yellow Sea, *Sci. Rep.*, 8(1), 1–12, <https://doi.org/10.1038/s41598-018-35309-3>, 2018.  
1085

1086 Vásquez-Elizondo, R. M., and Enríquez, S.: Light absorption in coralline algae (Rhodophyta): a  
1087 morphological and functional approach to understanding species distribution in a coral reef lagoon,  
1088 *Front. Mar. Sci.*, 4, 297, <https://doi.org/10.3389/fmars.2017.00297>, 2017.

1089 Vásquez-Elizondo, R. M., Legaria-Moreno, Pérez-Castro, M.A., Krämer, W. E., Scheufen, T.,

- 1090 Iglesias-Prieto, R., and Enríquez, S.: Absorbance determinations on multicellular tissues,  
1091 Photosynth. Res., 132, 311–324, <https://doi.org/10.1007/s11120-017-0395-6>, 2017.
- 1092 Velasco-Fuentes, O. V., and Marinone, S. G.: A numerical study of the Lagrangian circulation in the  
1093 Gulf of California, J. Mar. Syst., 22(1), 1–12. [https://doi.org/10.1016/S0924-7963\(98\)00097-9](https://doi.org/10.1016/S0924-7963(98)00097-9),  
1094 1999.
- 1095 Young, E. B., and Beardall, J.: Modulation of photosynthesis and inorganic carbon acquisition in a  
1096 marine microalga by nitrogen, iron, and light availability, Can. J. Bot., 83(7), 917–928,  
1097 <https://doi.org/10.1139/b05-081>, 2005.
- 1098 Young, J. N., Heureux, A. M., Sharwood, R. E., Rickaby, R. E., Morel, F. M., and Whitney, S. M.:  
1099 Large variation in the Rubisco kinetics of diatoms reveals diversity among their carbon-  
1100 concentrating mechanisms, J. Exp. Bot., 67(11), 3445–3456, <https://doi.org/10.1093/jxb/erw163>,  
1101 2016.
- 1102 Xu, J., Fan, X., Zhang, X., Xu, D., Mou, S., Cao, S., Zheng, Z., Miao, J., Ye, N.: Evidence of  
1103 coexistence of C<sub>3</sub> and C<sub>4</sub> photosynthetic pathways in a green-tide-forming alga, *Ulva prolifera*,  
1104 *PloS one*, 7(5), e37438, <https://doi.org/10.1371/journal.pone.0037438>, 2012.
- 1105 Xu, J., Zhang, X., Ye, N., Zheng, Z., Mou, S., Dong, M., Xu, D. and Miao, J.: Activities of principal  
1106 photosynthetic enzymes in green macroalga *Ulva linza*: functional implication of C<sub>4</sub> pathway in CO<sub>2</sub>  
1107 assimilation, Sci. China Life Sci., 56(6), 571–580, <https://doi.org/10.1007/s11427-013-4489-x>,  
1108 2013.
- 1109 Wefer, G., and Berger, W. H.: Stable isotope composition of benthic calcareous algae from Bermuda,  
1110 J. Sediment. Res., 51(2), 459–465, [https://doi.org/10.1306/212F7CAC-2B24-11D7-  
1111 8648000102C1865D](https://doi.org/10.1306/212F7CAC-2B24-11D7-8648000102C1865D), 1981.
- 1112 Wilkinson T. E., Wiken, J., Bezaury-Creel, T., Hourigan, T., Agardy, H., Herrmann, L., Janishevski,  
1113 C. Madden, L. Morgan and M. Padilla.: Marine Ecoregions of North America. CEC, Montreal,  
1114 Canada, 2009.
- 1115 Zabaleta, E., Martin, M. V., and Braun, H. P.: A basal carbon concentrating mechanism in plants?,  
1116 Plant Sci., 187, 97–104, <https://doi.org/10.1016/j.plantsci.2012.02.001>, 2012.

- 1117 Zeebe, R. E., and Wolf-Gladrow, D.: CO<sub>2</sub> in seawater: equilibrium, kinetics, isotopes (No. 65) Gulf  
1118 Professional Publishing, 2001.
- 1119 Zeitzschel, B.: Primary productivity in the Gulf of California, Mar. Biol., 3(3), 201–207,  
1120 <https://doi.org/10.1007/BF00360952>, 1969.
- 1121 Zou, D., Xia, J., and Yang, Y.: Photosynthetic use of exogenous inorganic carbon in the agarophyte  
1122 *Gracilaria lemaneiformis* (Rhodophyta), Aquac, 237, 421-431,  
1123 <https://doi.org/10.1016/j.aquaculture.2004.04.020>, 2004.
- 1124



1125 **Figure captions**

1126 Fig. 1. Sites collection along the continental (C1-C3) and peninsula (P1-P3) Gulf of California  
1127 coastlines (A), range of environmental factors supporting or limiting the life processes for the  
1128 macroalgal communities within a habitat (B), and inserted Table with the features and  
1129 environmental conditions in the diverse habitats in the GC bioregions that delimits the macroalgal  
1130 community's zonation.

1131 Fig. 2. Variability of  $\delta^{13}\text{C}$  values for specimens of different macroalgae genera collected along GC  
1132 coastlines classified by taxon: (A) Chlorophyta, (B) Ochrophyta and (C) Rhodophyta. Shaded  
1133 background represents the cutoff limits for using  $\text{CO}_2$  Only users and  $\text{HCO}_3^-$  only users,  
1134 respectively, according to Raven et al., (2002).

1135 Fig. 3. Variability of  $\delta^{13}\text{C}$  values for the genus collected along coastline of the Gulf of California  
1136 according to their taxon: (A) Chlorophyta, (B) Ochrophyta and (C) Rhodophyta. Genus with  $n=1$  is  
1137 not shown, and genus  $n=2$  was not considered to the statistical comparison. Different letters  
1138 indicate significant differences ( $P<0.05$ ):  $a>b>c>d>e$ . Shaded background represent the cutoff  
1139 limits for using  $\text{CO}_2$  Only users and  $\text{HCO}_3^-$  only users, respectively, according to Raven et al.,  
1140 (2002). For Chlorophyta: Bry= *Bryopsis*, Cau=*Caulerpa*, Cha= *Chaetomorpha*, Cla= *Cladophora*,  
1141 Cod= *Codium*, Phy= *Phyllocladon*, Str= *Struveopsis*, Ulv= *Ulva*. Phaeophyta: Col= *Colpomenia*,  
1142 Dic= *Dictyota*, Ect= *Ectocarpus*, End= *Endarachne*, Hyd= *Hydroclathrus*, Pad= *Padina*, Ros=  
1143 *Rosenvigea*, Sar= *Sargassum*, Spa= *Spatoglossum*, Zon= *zonaria*. Rhodophyta: Aca: *Acantophora*,  
1144 anf: *Anfeliopsis*, Amp= *Amphiroa*, Cen= *Centroceras*, Cer<sup>1</sup>= *Ceramium*, Cer<sup>2</sup>= *Ceratodictyon*,  
1145 Cho<sup>1</sup>= *Chondracanthus*, Cho<sup>2</sup>= *Chondria*, Das= *Dasya*, Dig= *Digenia*, Euc= *Euchema*, Gel=  
1146 *Gelidium*, Gig= *Gigartina*, Gra<sup>1</sup>= *Gracilaria*, Gra<sup>2</sup>= *Grateloupia*, Gra<sup>3</sup>= *Gracilariopsis*, Gym=

1147 *Gymnogongrus*, Hal= *Halymenia*, Hyp= *Hypnea*, Jan= *Jania*, Lau= *Laurencia*, Lom= *Lomentaria*,  
1148 Neo= *Neosiphonia*, Pol= *Polysiphonia*, Pri= *Prionitis*, Rho<sup>1</sup>= *Rhodoglossum*, Rho<sup>2</sup>=  
1149 *Rhodymenia*, Sch= *Schymenia*, Spy= *Spyridia*, Tac= *Tacanoosca*. Purple boxplots represent  
1150 calcifying species group.

1151 Fig. 4. Variability of  $\delta^{13}\text{C}$  values for morphofunctional groups by taxa along coastline of the Gulf  
1152 of California.

1153 Fig. 5 Proportion of species using different DIC sources according to their carbon uptake  
1154 strategies:  $\text{HCO}_3^-$  only users ( $\text{CO}_2$  concentrating mechanism active), Users of both sources ( $\text{HCO}_3^-$   
1155 &  $\text{CO}_2$ ) and  $\text{CO}_2$  only users (non- $\text{CO}_2$  concentrating mechanism active) in function of coast along  
1156 GC.

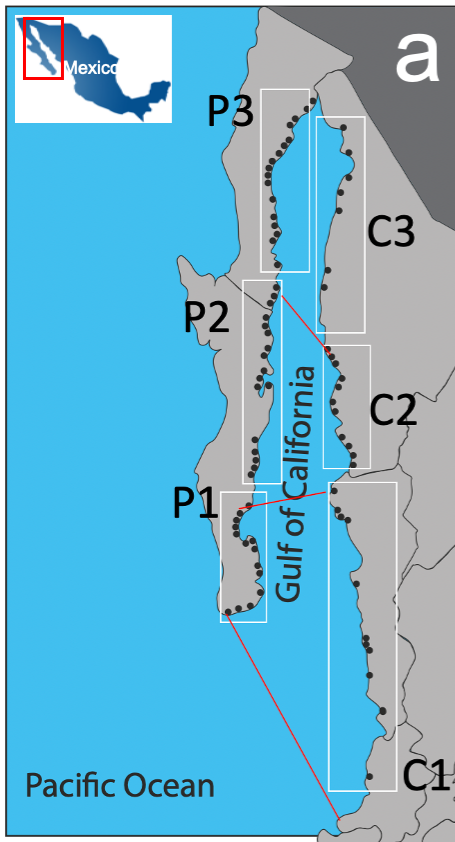
1157 Fig. 6. Variability of  $\delta^{13}\text{C}$  values in macroalgae specimens for the most representative genera in  
1158 function of habitat features (emersion level). Green circles represent genus of Chlorophyta, Brown  
1159 circles represent genus of Ochrophyta; red circles represent genus Rhodophyta and purple circles  
1160 represent genus with calcifying capacity.

1161 Fig. 7. Variability of  $\delta^{13}\text{C}$  values in macroalgae specimens for the most representative genus in  
1162 function of temperature (a) and pH (b) ranges in samples collected along Gulf of California  
1163 coastline.

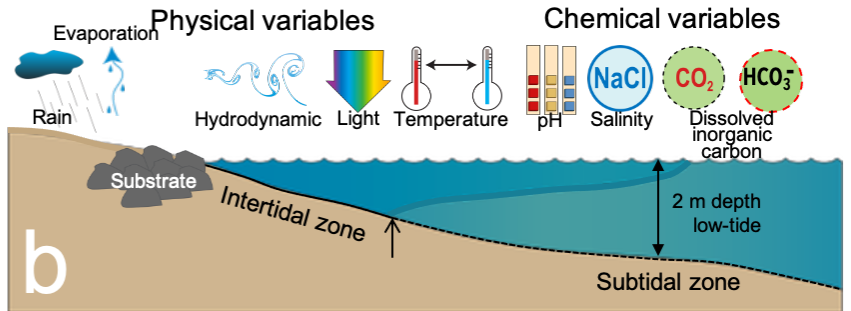
1164 Fig. 8. Proportion of species using different DIC sources according to their carbon assimilation  
1165 strategies:  $\text{HCO}_3^-$  only users ( $\text{CO}_2$  concentrating mechanism active), Users of both sources ( $\text{HCO}_3^-$   
1166 &  $\text{CO}_2$ ) and  $\text{CO}_2$  only users (non- $\text{CO}_2$  concentrating mechanism active) in function of : (A) pH  
1167 ranges, (B) temperature ranges and (C) salinity ranges.

1168 Fig. 9. Trends in the  $\delta^{13}\text{C}$ -macroalgal in specimens collected along continental (C1-C3) and  
1169 peninsula (P1-P3) Gulf of California coastline in function of latitudinal gradient.

1170



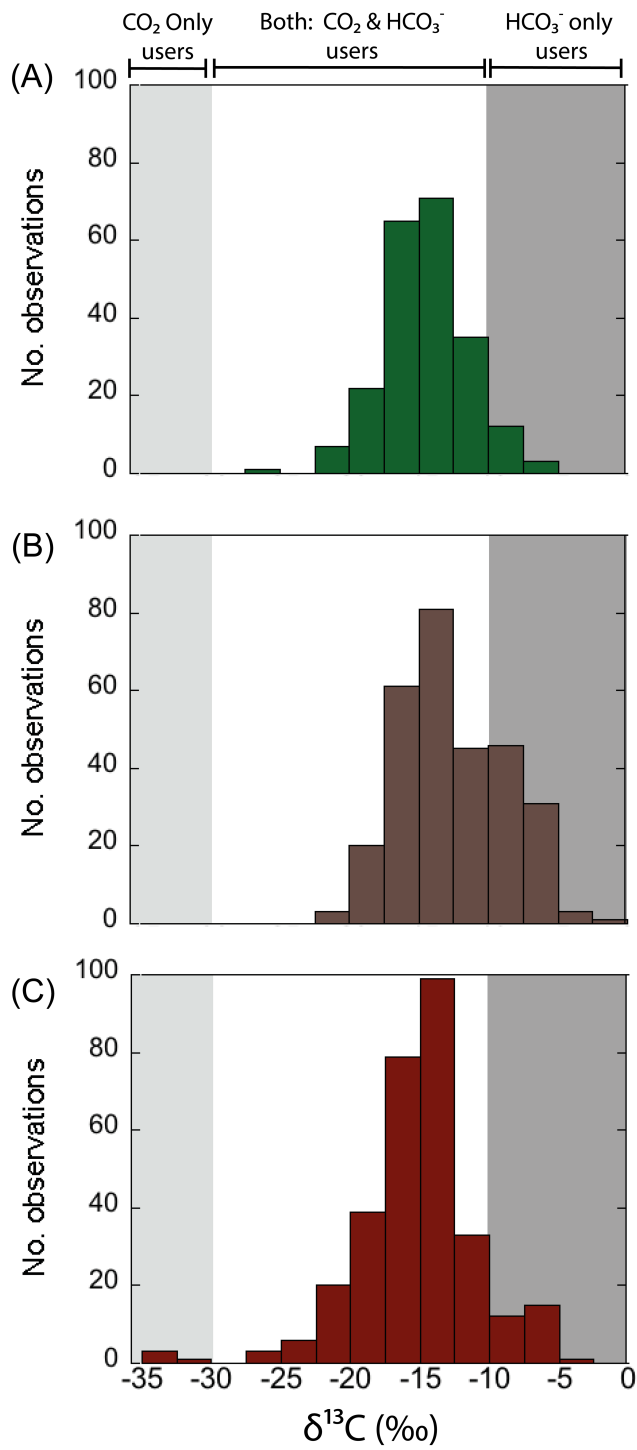
Habitats features and environmental conditions in sampling sites



| Environmental factors         | Continental GC coastline   |                                |                            | Peninsula GC coastline     |                            |                            |
|-------------------------------|----------------------------|--------------------------------|----------------------------|----------------------------|----------------------------|----------------------------|
|                               | C1                         | C2                             | C3                         | P1                         | P2                         | P3                         |
| Substrate at shores           | Rocky and sandy-rocky      | Only sandy-rocky shore         | Rocky and sandy-rocky      | Rocky and sandy-rocky      | Rocky and sandy-rocky      | Rocky and sandy-rocky      |
| Hydrodynamic (water movement) | Slow to fast               | Slow to fast                   | Slow to fast               | Slow to fast               | Slow to fast               | Slow to fast               |
| Protection level sites        | Exposed and protected      | Exposed and protected          | Exposed and protected      | Exposed and protected      | Exposed and protected      | Exposed and protected      |
| Immersion level               | Intertidal and subtidal    | Intertidal and subtidal        | Intertidal and subtidal    | Intertidal and subtidal    | Intertidal and subtidal    | Intertidal and subtidal    |
| pH ranges                     | Acid, typical and alkaline | Acid, typical and alkaline     | Acid, typical and alkaline | Acid, typical and alkaline | Typical and alkaline       | Acid, typical and alkaline |
| Temperature ranges            | Typical and warmer         | Colder, typical and warmer     | Colder, typical and warmer | Colder, typical and warmer | Colder, typical and warmer | Colder, typical and warmer |
| Salinity ranges               | Marine                     | Hypersaline, marine, estuarine | Marine                     | Marine                     | Marine                     | Marine                     |

1171

1172 Fig. 1



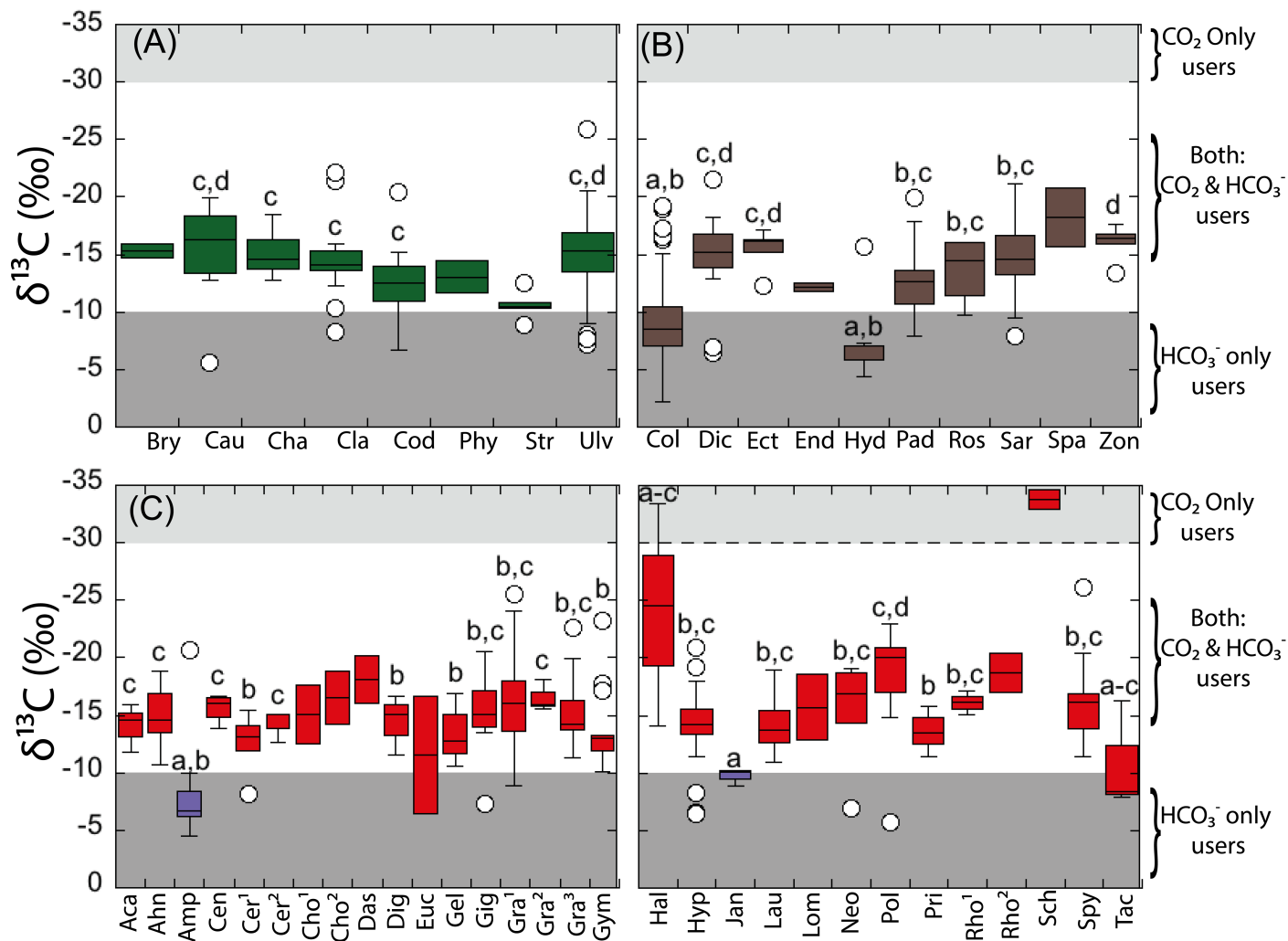
1173

1174 Fig 2

1175

1176

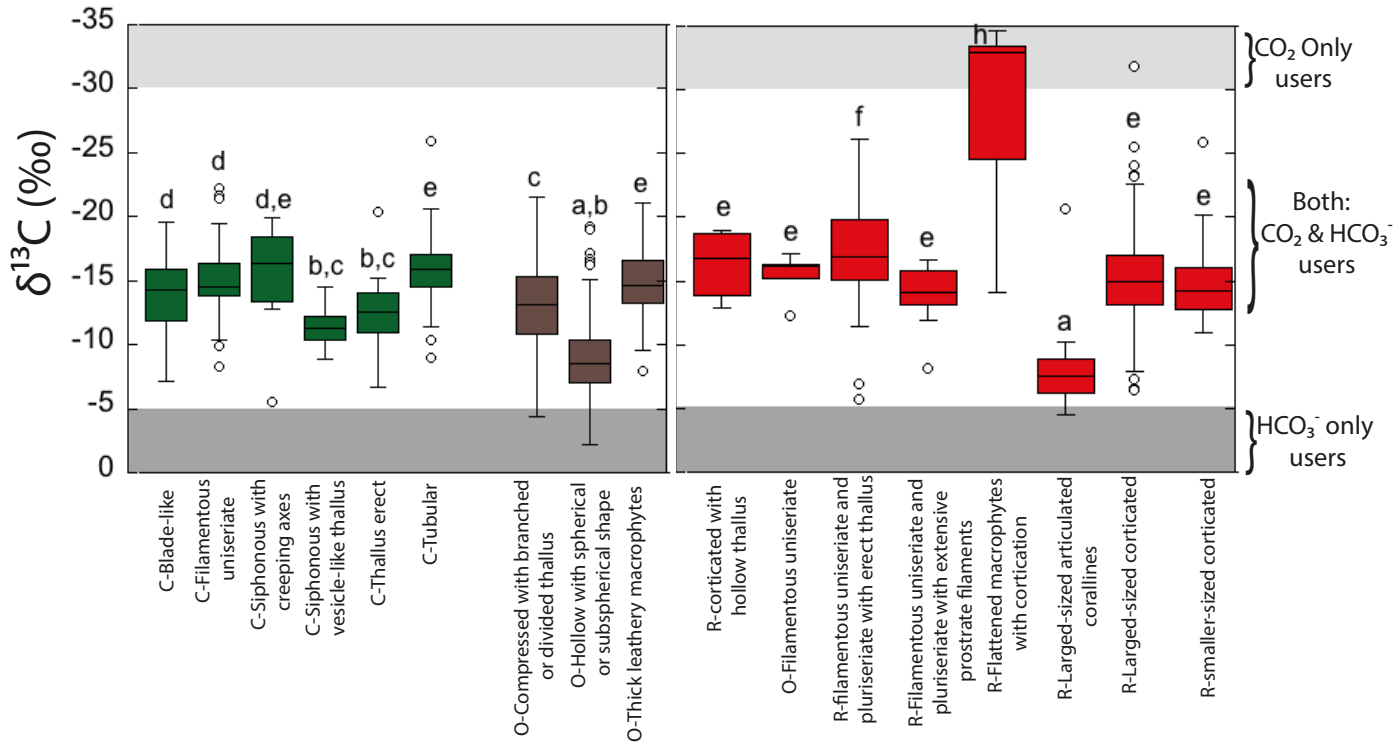
1177



1178

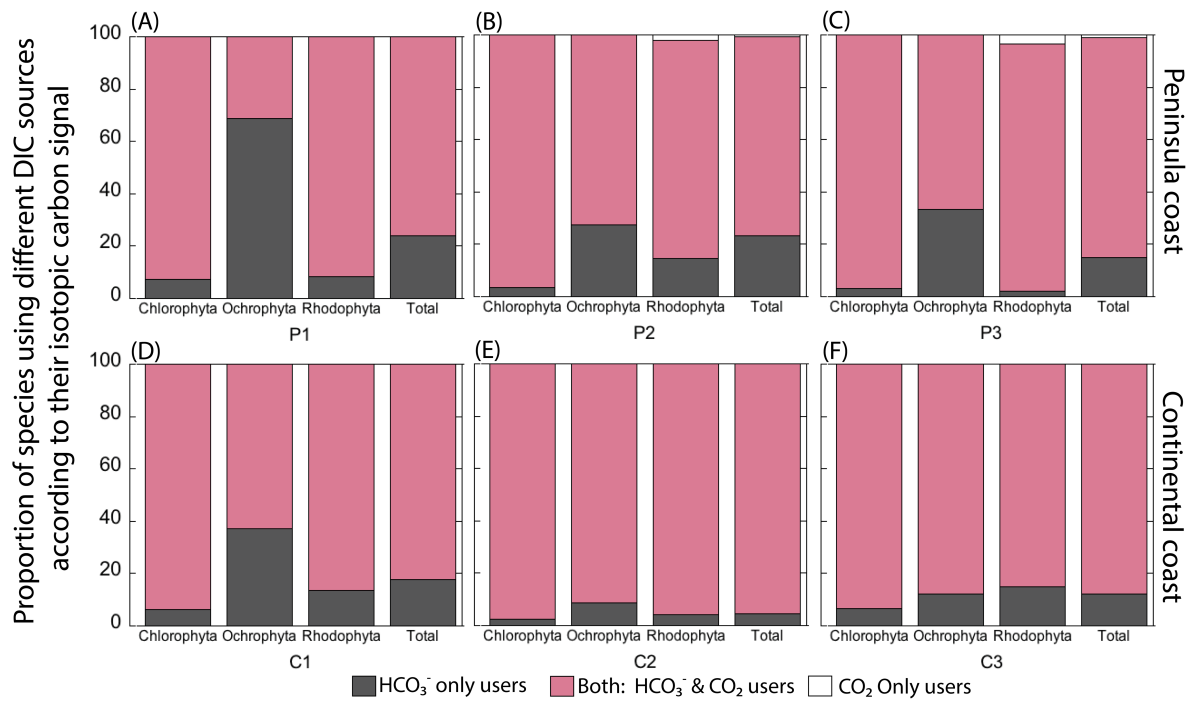
1179

Fig 3



1180

1181 **Fig 4**

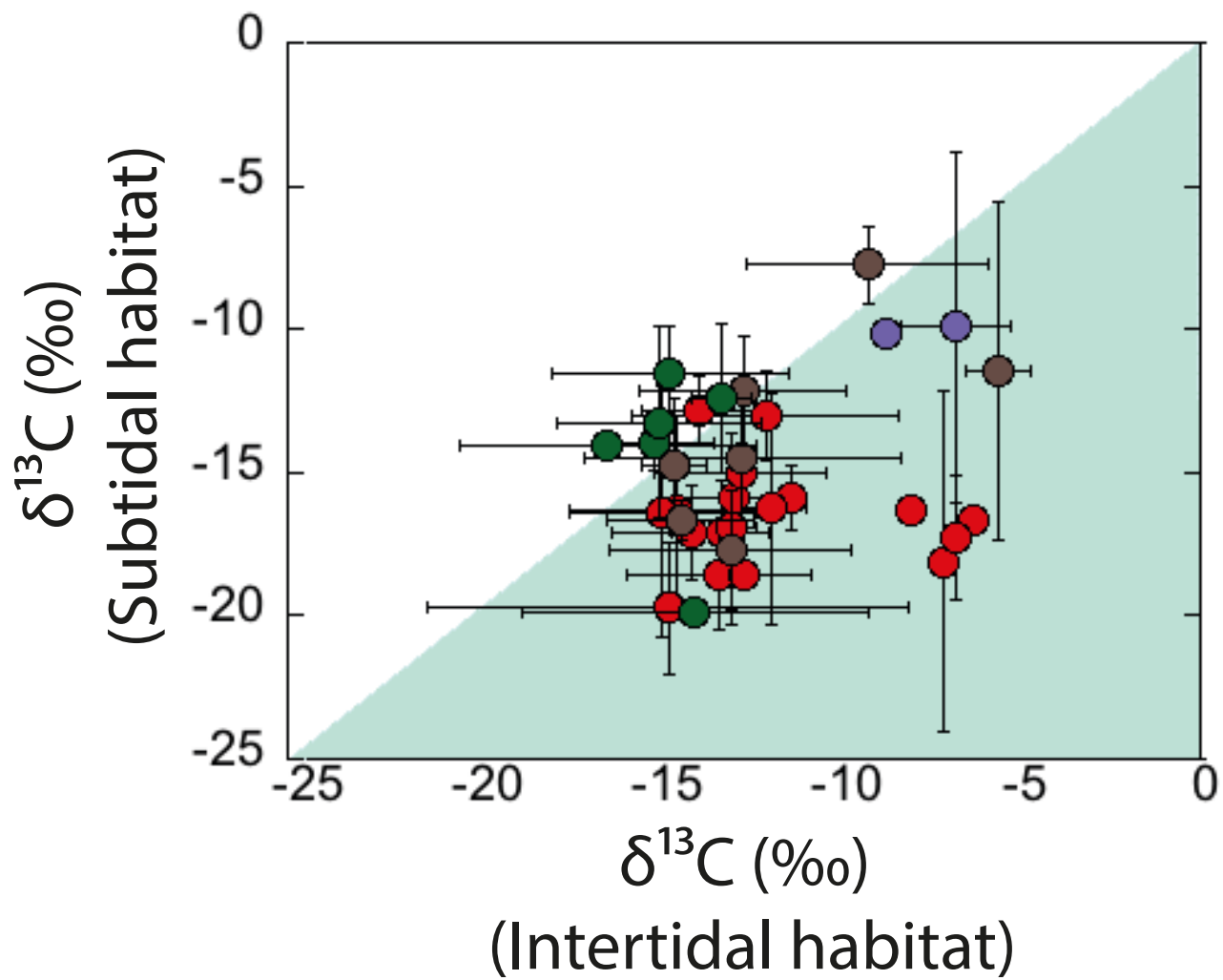


1182

1183 **Fig 5**

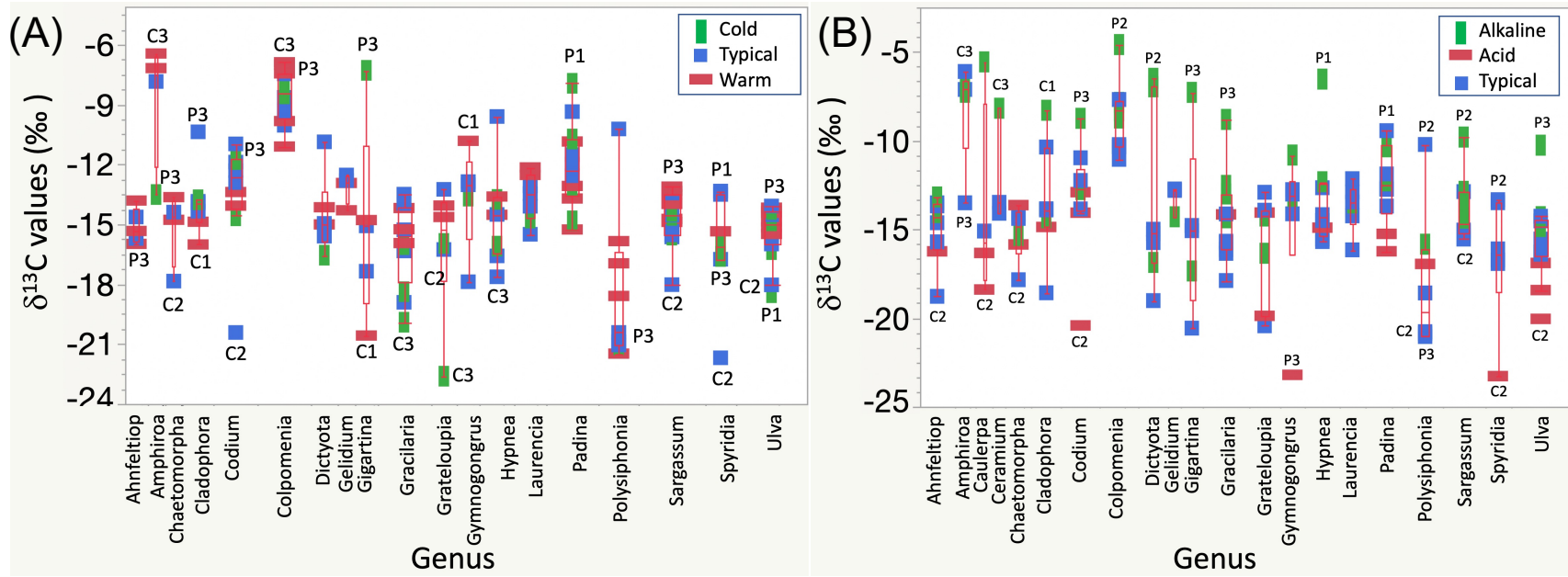


1184



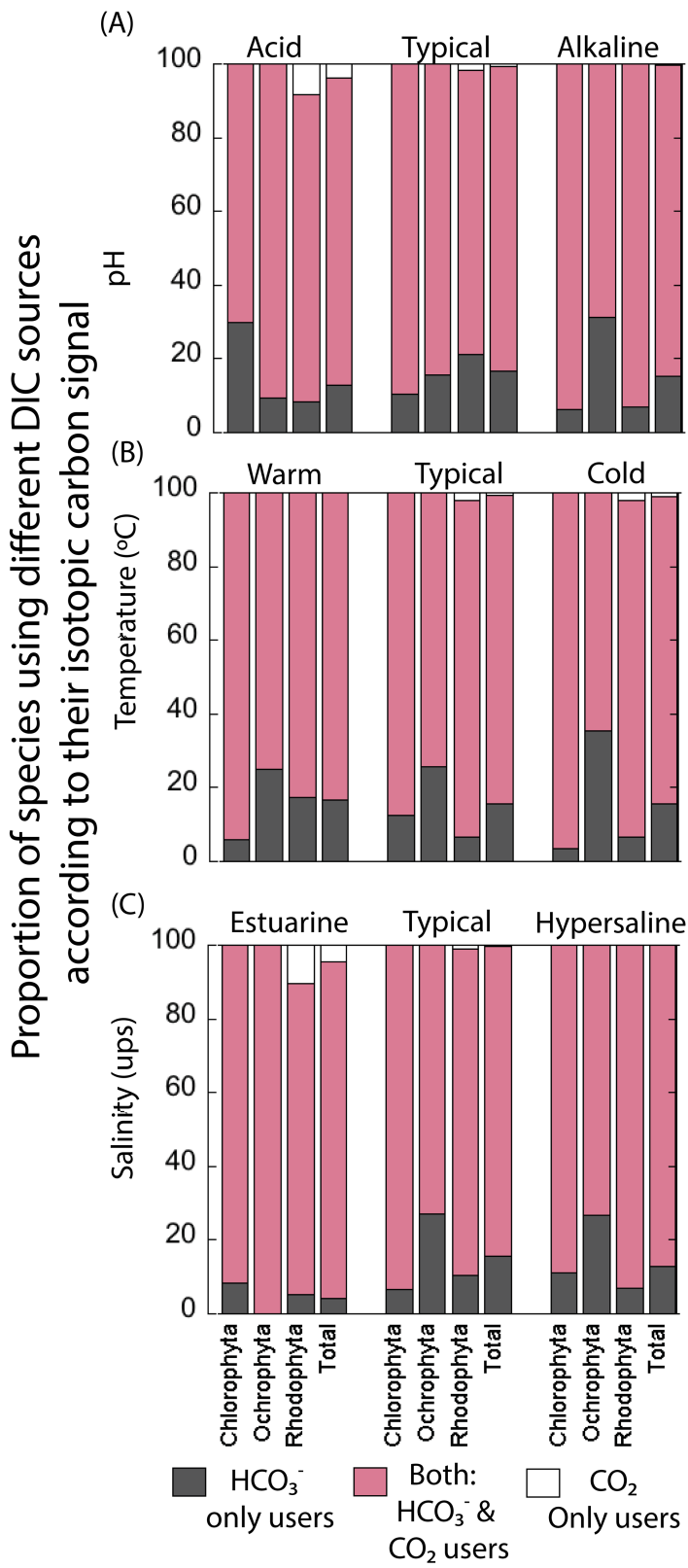
1185

1186 **Fig 6**



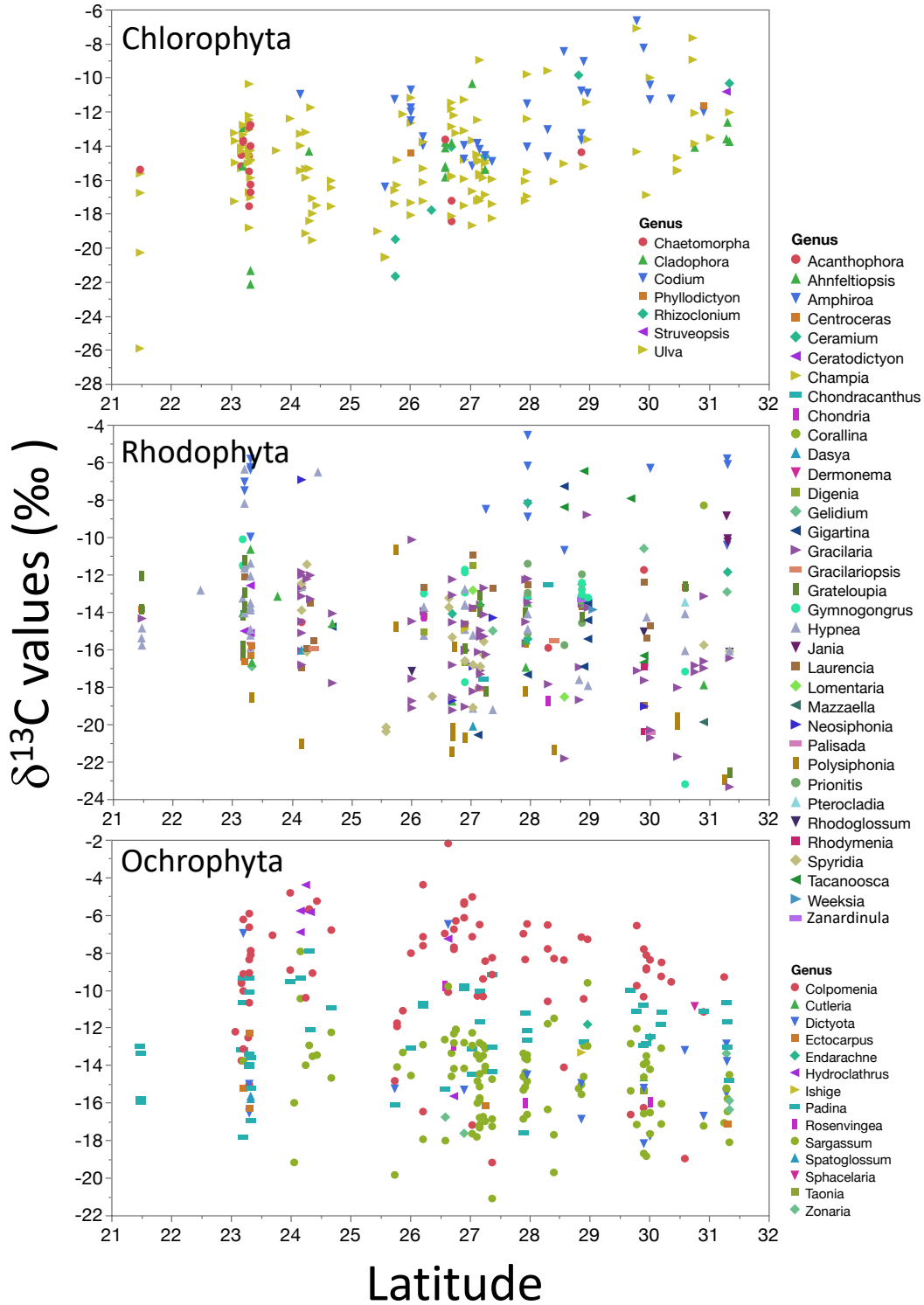
1187

1188 **Fig 7**



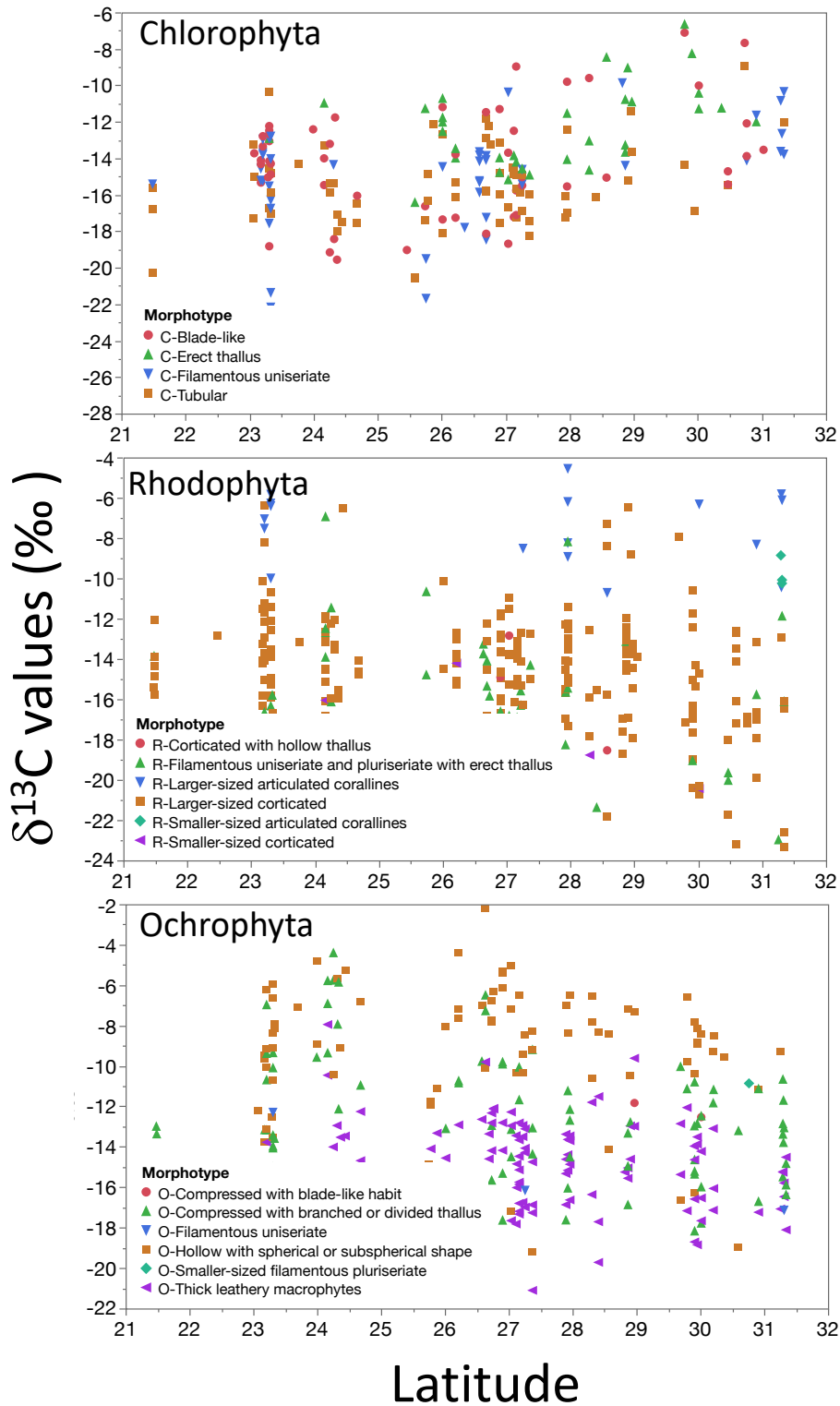
1189

1190 **Fig 8**



1191

1192 **Fig. 9**



1193

1194 **Fig. 10**

Table 1. Carbon isotopic composition (‰) in species of Phyla Chlorophyta collected along Gulf of California coastlines.

| Species (n composite samples)  | $\delta^{13}\text{C} \pm \text{SD}$ (Min to Max, ‰) |
|--------------------------------|---|
| <i>Chaetomorpha</i> sp. (3)    | -13.7 $\pm$ 0.8 (-14.6 to -12.9)                    |
| <i>C. antennina</i> (10)       | -14.6 $\pm$ 1.1 (-16.3 to -12.8)                    |
| <i>C. linum</i> (5)            | -16.8 $\pm$ 1.6 (-18.5 to -14.6)                    |
| <i>Codium</i> sp. (5)          | -11.6 $\pm$ 3.0 (-14.1 to -6.7)                     |
| <i>C. amplivesiculatum</i> (8) | -14.4 $\pm$ 2.7 (-20.4 to -11.3)                    |
| <i>C. brandegeei</i> (7)       | -11.8 $\pm$ 1.2 (-13.7 to -10.4)                    |
| <i>C. fragile</i> (4)          | -13.0 $\pm$ 2.7 (-14.8 to -9.0)                     |
| <i>C. simulans</i> (9)         | -11.4 $\pm$ 2.2 (-14.9 to -8.3)                     |
| <i>Ulva</i> sp. (12)           | -14.0 $\pm$ 3.9 (-19.2 to -7.1)                     |
| <i>U. acanthophora</i> (25)    | -15.8 $\pm$ 1.7 (-18.3 to -11.4)                    |
| <i>U. clathrata</i> (8)        | -16.4 $\pm$ 2.0 (-20.5 to -14.5)                    |
| <i>U. compressa</i> (4)        | -17.8 $\pm$ 2.4 (-20.6 to -15.4)                    |
| <i>U. flexuosa</i> (13)        | -16.0 $\pm$ 3.7 (-25.9 to -10.4)                    |
| <i>U. intestinalis</i> (16)    | -15.3 $\pm$ 2.5 (-20.3 to -8.9)                     |
| <i>U. lactuca</i> (31)         | -14.1 $\pm$ 3.1 (-19.6 to -7.7)                     |
| <i>U. linza</i> (6)            | -15.6 $\pm$ 2.4 (-19.4 to -13.2)                    |
| <i>U. lobata</i> (5)           | -13.2 $\pm$ 1.9 (-15.3 to -11.1)                    |
| <i>U. prolifera</i> (3)        | -14.2 $\pm$ 1.8 (-15.5 to -12.2)                    |

Table 2. Carbon isotopic composition (‰) in species of Phyla Ochrophyta collected along Gulf of California coastlines.

| Species (n composite samples) | $\delta^{13}\text{C} \pm \text{SD}$ (Min to Max, ‰) |
|-------------------------------|---|
| <i>Colpomenia</i> sp. (11)    | -11.0 $\pm$ 3.7 (-19.0 to -5.4)                     |
| <i>C. ramosa</i> (4)          | -11.4 $\pm$ 2.6 (-13.8 to -7.8)                     |
| <i>C. sinuosa</i> (7)         | -10.2 $\pm$ 3.0 (-16.3 to -7.2)                     |
| <i>C. tuberculata</i> (64)    | -8.7 $\pm$ 3.2 (-19.2 to -2.2)                      |
| <i>Padina</i> sp. (15)        | -11.1 $\pm$ 1.5 (-13.1 to -7.9)                     |
| <i>P. crispata</i> (3)        | -11.3 $\pm$ 1.7 (-12.5 to -10.1)                    |
| <i>P. durvillaei</i> (36)     | -13.2 $\pm$ 2.6 (-20.0 to -9.2)                     |
| <i>Sargassum</i> sp. (34)     | -14.3 $\pm$ 2.4 (-18.7 to -8.0)                     |
| <i>S. herporhizum</i> (7)     | -13.7 $\pm$ 1.6 (-16.6 to -11.5)                    |
| <i>S. horridum</i> (12)       | -15.5 $\pm$ 2.9 (-19.7 to -9.5)                     |
| <i>S. johnstonii</i> (10)     | -15.4 $\pm$ 2.0 (-17.7 to -11.8)                    |
| <i>S. lapazeanum</i> (7)      | -14.49 $\pm$ 1.59 (-17.2 to -12.8)                  |
| <i>S. sinicola</i> (31)       | -15.1 $\pm$ 2.4 (-21.1 to -12.1)                    |

1196

1197 Table 3. Carbon isotopic composition (‰) in species of Phyla Rhodophyta collected along Gulf of  
 1198 California coastlines.

| Species (n composite samples)  | $\delta^{13}\text{C} \pm \text{SD}$ (Min to Max, ‰) |
|--------------------------------|---|
| <i>Gracilaria</i> sp. (18)     | -15.5 $\pm$ 2.4 (-21.8 to -12.2)                    |
| <i>Gracilaria</i> sp.2 (3)     | -14.4 $\pm$ 3.7 (-18.7 to -12.3)                    |
| <i>G. crispata</i> (7)         | -15.1 $\pm$ 3.0 (-19.1 to -10.1)                    |
| <i>G. pacifica</i> (6)         | -16.5 $\pm$ 1.6 (-18.6 to -13.6)                    |
| <i>G. spinigera</i> (3)        | -14.9 $\pm$ 3.8 (-17.7 to -12.2)                    |
| <i>G. subsecundata</i> (8)     | -15.9 $\pm$ 2.8 (-20.3 to -12.8)                    |
| <i>G. tepocensis</i> (3)       | -15.1 $\pm$ 1.9 (-17.0 to -13.2)                    |
| <i>G. textorii</i> (4)         | -16.2 $\pm$ 2.6 (-18.1 to -14.3)                    |
| <i>G. turgida</i> (5)          | -15.3 $\pm$ 3.6 (-20.7 to -12.0)                    |
| <i>G. vermiculophylla</i> (16) | -15.9 $\pm$ 3.8 (-23.4 to -8.8)                     |
| <i>Hypnea</i> sp. (14)         | -14.9 $\pm$ 2.6 (-20.9 to -11.4)                    |
| <i>H. johnstonii</i> (5)       | -11.2 $\pm$ 3.5 (-13.8 to -6.5)                     |
| <i>H. pannosa</i> (5)          | -11.8 $\pm$ 3.3 (-15.0 to -6.4)                     |
| <i>H. spinella</i> (6)         | -16.4 $\pm$ 1.8 (-19.2 to -14.9)                    |
| <i>H. valentiae</i> (6)        | -15.2 $\pm$ 2.3 (-19.2 to -12.7)                    |
| <i>Laurencia</i> sp. (8)       | -12.9 $\pm$ 1.2 (-14.7 to -10.5)                    |
| <i>L. pacifica</i> (8)         | -14.9 $\pm$ 2.2 (-19.0 to -12.7)                    |
| <i>L. papillosa</i> (3)        | -15.7 $\pm$ 0.3 (-15.9 to -15.6)                    |
| <i>Spyrida</i> sp. (5)         | -17.1 $\pm$ 1.12 (-19.1 to -16.1)                   |
| <i>S. filamentosa</i> (14)     | -15.9 $\pm$ 3.8 (-26.2 to -11.5)                    |

1199

1200

1201



1202 Table 4. Summary of the estimated regression coefficients for each simple linear regression  
 1203 analyses and on the constant of fitted regression models. Estimated regression coefficients includes  
 1204 degrees of freedom for the error (DFE), root-mean-square error (RMSE), coefficients of  
 1205 determination ( $R^2$ ) and the adjusted  $R^2$  statistics, Mallow's Cp criterion (Cp), Akaike Information  
 1206 Criterion (AIC), Bayesian Information Criterion (BIC) minimum, F Ratio test, and p-value for the  
 1207 test (Prob > F). Models information includes value of the constant a ( $\delta^{13}C$ , ‰), standard error (SE),  
 1208 t ratio and Prob > |t| (values \* are significant).

| Independent variables           | Estimated regression coefficients |      |       |              |     |       |       |         | Model constant (a) |                    |      |         |           |
|---------------------------------|-----------------------------------|------|-------|--------------|-----|-------|-------|---------|--------------------|--------------------|------|---------|-----------|
|                                 | DFE                               | RMSE | $R^2$ | Adjust $R^2$ | Cp  | AICc  | BIC   | F ratio | Prob > F           | $\delta^{13}C$ (‰) | SE   | t ratio | Prob >  t |
| Inherent macroalgae properties  |                                   |      |       |              |     |       |       |         |                    |                    |      |         |           |
| Phyla                           | 806                               | 3.66 | 0.08  | 0.07         | 3   | 4,401 | 4,420 | 33.1    | <.0001**           | -13.98             | 0.13 | -107.4  | <.0001**  |
| Morphofunctional                | 788                               | 3.10 | 0.35  | 0.34         | 21  | 4,149 | 4,251 | 21.6    | <.0001**           | -14.21             | 0.35 | -40.80  | <.0001**  |
| Genus                           | 746                               | 2.92 | 0.46  | 0.41         | 63  | 4,104 | 4,393 | 10.1    | <.0001**           | -14.71             | 0.23 | -62.64  | <.0001*   |
| Species                         | 641                               | 2.79 | 0.57  | 0.46         | 168 | 4,195 | 4,898 | 5.2     | <.0001**           | -14.60             | 0.16 | -93.22  | <.0001**  |
| Biogeographical collection zone |                                   |      |       |              |     |       |       |         |                    |                    |      |         |           |
| GC coastline                    | 807                               | 3.79 | 0.01  | 0.01         | 2   | 4,456 | 4,470 | 7.4     | 0.0067*            | -13.97             | 0.13 | -104.5  | <.0001**  |
| Coastal sector                  | 803                               | 3.73 | 0.05  | 0.04         | 6   | 4,433 | 4,465 | 7.9     | <.0001*            | -14.12             | 0.16 | -90.85  | <.0001**  |
| Latitude                        | 807                               | 3.80 | 0.00  | 0.00         | 2   | 4,462 | 4,476 | 1.5     | 0.23               | -12.25             | 1.41 | -8.71   | <.0001**  |
| Longitude                       | 807                               | 3.81 | 0.00  | 0.00         | 2   | 4,463 | 4,477 | 0.1     | 0.80               | -15.44             | 5.83 | -2.65   | 0.0082*   |
| Habitat features                |                                   |      |       |              |     |       |       |         |                    |                    |      |         |           |
| Substrate                       | 807                               | 3.80 | 0.00  | 0.00         | 2   | 4,460 | 4,474 | 3.2     | 0.08               | -13.82             | 0.15 | -92.06  | <.0001*   |
| Hydrodynamic                    | 807                               | 3.80 | 0.00  | 0.00         | 2   | 4,462 | 4,476 | 1.3     | 0.26               | -13.88             | 0.15 | -95.00  | <.0001**  |
| Emersion level                  | 807                               | 3.69 | 0.06  | 0.06         | 2   | 4,412 | 4,427 | 52.2    | <.0001**           | -14.05             | 0.13 | -107.6  | <.0001**  |
| Environmental conditions        |                                   |      |       |              |     |       |       |         |                    |                    |      |         |           |
| Temperature                     | 802                               | 3.70 | 0.01  | 0.01         | 2   | 4,390 | 4,404 | 5.4     | 0.0207*            | -16.11             | 0.96 | -16.78  | <.0001*   |
| pH                              | 807                               | 3.73 | 0.04  | 0.04         | 2   | 4,430 | 4,444 | 33.4    | <.0001**           | -32.45             | 3.21 | -10.13  | <.0001**  |
| Salinity                        | 806                               | 3.80 | 0.00  | 0.00         | 2   | 4,456 | 4,470 | 0.9     | 0.34               | -15.77             | 1.91 | -8.27   | <.0001**  |

1209 \*p<0.05, \*\*p<0.0001

1210 Table 5. Summary of the estimated regression coefficients for each multivariate linear  
 1211 regression analyses and on their constant of fitted regression models performed in  
 1212 individuals binned by genus. Estimated regression coefficients include degrees of freedom  
 1213 for the error (DFE), root-mean-square error (RMSE), coefficients of determination ( $R^2$ ) and  
 1214 the adjusted  $R^2$  statistics, Mallows' Cp criterion (Cp), Akaike Information Criterion (AIC),  
 1215 Bayesian Information Criterion (BIC) minimum, F Ratio test, and p-value for the test (Prob  
 1216 > F). Model information includes value of the constant a ( $\delta^{13}\text{C}$ , ‰), standard error (SE), t  
 1217 ratio and Prob > |t| (values \* are significant).

| Independent variables | Estimated regression coefficients |      |       |              |     |       |       |         | Model constant (a) |                           |      |         |           |
|-----------------------|-----------------------------------|------|-------|--------------|-----|-------|-------|---------|--------------------|---------------------------|------|---------|-----------|
|                       | DFE                               | RMSE | $R^2$ | Adjust $R^2$ | Cp  | AICc  | BIC   | F ratio | Prob > F           | $\delta^{13}\text{C}$ (‰) | SE   | t ratio | Prob >  t |
| Coastal sector        | 652                               | 2.78 | 0.57  | 0.47         | 157 | 4,169 | 4,834 | 20.0    | <.0001*            | -17.52                    | 0.64 | -27.24  | <.0001*   |
| Substrate             | 711                               | 2.90 | 0.49  | 0.42         | 98  | 4,140 | 4,577 | 0.4     | 0.52               | -16.35                    | 0.62 | -26.20  | <.0001*   |
| Hydrodynamic          | 714                               | 2.87 | 0.50  | 0.43         | 95  | 4,120 | 4,545 | 0.1     | 0.78               | -16.53                    | 0.64 | -25.95  | <.0001*   |
| Emersion level        | 713                               | 2.77 | 0.53  | 0.47         | 96  | 4,060 | 4,489 | 153.0   | <.0001*            | -16.65                    | 0.60 | -27.85  | <.0001*   |
| Temperature           | 695                               | 2.81 | 0.50  | 0.43         | 109 | 4,083 | 4,564 | 98.4    | <.0001*            | -14.60                    | 0.92 | -15.91  | <.0001*   |
| Temperature ranges    | 686                               | 2.87 | 0.49  | 0.40         | 118 | 4,128 | 4,645 | 97.7    | <.0001*            | -12.91                    | 0.40 | -31.97  | <.0001*   |
| pH                    | 701                               | 2.86 | 0.51  | 0.43         | 108 | 4,134 | 4,611 | 156.6   | <.0001*            | -28.57                    | 2.69 | -10.64  | <.0001*   |
| pH ranges             | 697                               | 2.67 | 0.57  | 0.51         | 112 | 4,028 | 4,522 | 152.2   | <.0001*            | -16.39                    | 0.58 | -28.05  | <.0001*   |
| Salinity              | 697                               | 2.89 | 0.50  | 0.42         | 111 | 4,151 | 4,640 | 162.2   | <.0001*            | -17.75                    | 1.63 | -10.88  | <.0001*   |
| Salinity ranges       | 721                               | 2.91 | 0.47  | 0.41         | 86  | 4,117 | 4,504 | 167.8   | <.0001*            | -17.64                    | 0.74 | -23.68  | <.0001*   |

1218

1219

1220

1221

1222

1223

1224 Table 6. Summary of the estimated regression coefficients for each multivariate linear regression  
 1225 analyses and on their constant of fitted regression models performed in individuals binned by  
 1226 coastline sector and genus. Estimated regression coefficients include degrees of freedom for the  
 1227 error (DFE), root-mean-square error (RMSE), coefficients of determination ( $R^2$ ) and the adjusted  
 1228  $R^2$  statistics, Mallows' Cp criterion (Cp), Akaike Information Criterion (AIC), Bayesian  
 1229 Information Criterion (BIC) minimum, F Ratio test, and p-value for the test (Prob > F). Model  
 1230 information includes value of the constant a ( $\delta^{13}C$ , ‰), standard error (SE), t ratio and Prob > |t|  
 1231 (values \* are significant).

| Independent variables | DFE | RMSE | Estimated regression coefficients |                       |     |       |       |         | Prob > F | Model constant (a) |      |         |           |
|-----------------------|-----|------|-----------------------------------|-----------------------|-----|-------|-------|---------|----------|--------------------|------|---------|-----------|
|                       |     |      | R <sup>2</sup>                    | Adjust R <sup>2</sup> | Cp  | AICc  | BIC   | F ratio |          | $\delta^{13}C$ (‰) | SE   | t ratio | Prob >  t |
| Substrate             | 590 | 2.76 | 0.62                              | 0.47                  | 219 | 4,287 | 5,155 | 15.8    | <.0001*  | -17.08             | 0.66 | -25.72  | <.0001*   |
| Hydrodynamic          | 592 | 2.73 | 0.62                              | 0.49                  | 217 | 4,266 | 5,128 | 18.6    | <.0001*  | -17.18             | 0.67 | -25.70  | <.0001*   |
| Protection level      | 590 | 2.75 | 0.62                              | 0.48                  | 219 | 4,285 | 5,153 | 20.0    | <.0001*  | -17.51             | 0.64 | -27.22  | <.0001*   |
| Emersion level        | 603 | 2.69 | 0.63                              | 0.50                  | 206 | 4,217 | 5,045 | 18.6    | <.0001*  | -17.47             | 0.64 | -27.49  | <.0001*   |
| Temperature ranges    | 569 | 2.74 | 0.61                              | 0.46                  | 235 | 4,293 | 5,202 | 28.0    | <.0001*  | -13.73             | 0.45 | -30.32  | <.0001*   |
| pH ranges             | 580 | 2.50 | 0.69                              | 0.57                  | 229 | 4,155 | 5,051 | 9.7     | 0.0019*  | -16.88             | 0.62 | -27.15  | <.0001*   |
| Salinity ranges       | 631 | 2.76 | 0.58                              | 0.47                  | 176 | 4,183 | 4,913 | 21.2    | <.0001*  | -18.30             | 0.79 | -23.05  | <.0001*   |

1233

1234 Table 7. Summary of the estimated regression coefficients for each multivariate linear regression  
 1235 analyses and on their constant of fitted regression models performed in individuals binned in  
 1236 coastline sector, habitats features, environmental conditions, and Physiological performed  
 1237 separately by morpho-functional groups and genus. Estimated regression coefficients include  
 1238 degrees of freedom for the error (DFE), root-mean-square error (RMSE), coefficients of  
 1239 determination ( $R^2$ ) and the adjusted  $R^2$  statistics, Mallows'  $C_p$  criterion ( $C_p$ ), Akaike Information  
 1240 Criterion (AIC), Bayesian Information Criterion (BIC) minimum, F Ratio test, and p-value for the  
 1241 test (Prob > F). Model information includes value of the constant a ( $\delta^{13}C$ , ‰), standard error (SE),  
 1242 t ratio and Prob > |t| (values \* are significant).

| Full model   | Estimated regression coefficients |      |       |              |       |       |       |         | Model constant (a) |                    |      |         |           |
|--|-----------------------------------|------|-------|--------------|-------|-------|-------|---------|--------------------|--------------------|------|---------|-----------|
|  | DFE                               | RMSE | $R^2$ | Adjust $R^2$ | $C_p$ | AICc  | BIC   | F ratio | Prob > F           | $\delta^{13}C$ (‰) | SE   | t ratio | Prob >  t |
| Coastline sector + Habitats features + Morphofunctional group        |                                   |      |       |              |       |       |       |         |                    |                    |      |         |           |
| I-Morpho-functional  | 593                               | 2.79 | 0.60  | 0.46         | 216   | 4,301 | 5,160 | 20.8    | <.0001*            | -13.49             | 0.57 | -23.52  | <.0001*   |
| Coastline sector + Environmental conditions + Morphofunctional group |                                   |      |       |              |       |       |       |         |                    |                    |      |         |           |
| II-Morpho-functional   | 680                               | 2.90 | 0.51  | 0.42         | 129   | 4,189 | 4,750 | 25.1    | <.0001*            | -13.42             | 0.54 | -24.74  | <.0001*   |
| Coastline sector + Habitat features+ Genus                           |                                   |      |       |              |       |       |       |         |                    |                    |      |         |           |
| I-Genus  | 482                               | 2.66 | 0.71  | 0.51         | 327   | 4,565 | 5,655 | 15.8    | <.0001*            | -16.93             | 0.73 | -23.27  | <.0001*   |
| Coastline sector + Environmental conditions + Genus                  |                                   |      |       |              |       |       |       |         |                    |                    |      |         |           |
| II-Genus   | 494                               | 2.49 | 0.72  | 0.55         | 310   | 4,374 | 5,438 | 14.8    | 0.0001*            | -13.55             | 0.64 | -21.17  | <.0001*   |

1243

1244 Table 8. Constant of fitted regression model explaining the  $\delta^{13}\text{C}$  variability by morpho-functional  
 1245 groups. Model information includes value of the constant a ( $\delta^{13}\text{C}$ , ‰), standard error (SE), t ratio  
 1246 and Prob > |t|. Only morpho-functional groups with significant effects are enlisted.

| Term  | Estimated | SE  | Razón t | Prob >  t |
|---|-----------|-----|---------|-----------|
| Model constant                                    | -14.2     | 0.4 | -40.80  | <.0001**  |
| R-Smaller-sized articulated corallines            | 4.5       | 1.7 | 2.58    | 0.0100*   |
| O-Compressed with branched or divided thallus     | 1.2       | 0.5 | 2.66    | 0.0079*   |
| C-Erect thallus                                   | 1.8       | 0.6 | 2.84    | 0.0046*   |
| R-Larger-sized articulated corallines             | 6.3       | 0.8 | 7.95    | <.0001*   |
| O-Hollow with spherical or subspherical shape     | 5.0       | 0.5 | 10.51   | <.0001*   |
| R-Blade-like with one of few layers of cells      | -5.9      | 3.0 | -1.98   | 0.0476*   |
| C-Tubular   | -1.6      | 0.5 | -3.26   | 0.0012**  |
| R-Filamentous uni&pluriseriate with erect thallus | -2.2      | 0.6 | -3.92   | <.0001*   |
| R-Flattened macrophytes with cortication          | -8.9      | 1.3 | -7.10   | <.0001*   |

1247 \*p<0.05, \*\*p<0.0001

1248

1249

1250

1251

1252

1253

1254

1255

1256 Table 9. Constant of fitted regression model explaining the  $\delta^{13}\text{C}$  variability by genus. Model  
 1257 information includes value of the constant a ( $\delta^{13}\text{C}$ , ‰), standard error (SE), t ratio and Prob > |t|.   
 1258 Only genus with significant effects are enlisted.

| Term                 | Estimated | SE  | Razón t | Prob >  t |
|----------------------|-----------|-----|---------|-----------|
| Model constant       | -14.7     | 0.2 | -62.64  | <.0001**  |
| <i>Corallina</i>     | 6.4       | 2.9 | 2.22    | 0.0269*   |
| <i>Tacanoosca</i>    | 3.5       | 1.3 | 2.71    | 0.0070*   |
| <i>Jania</i>         | 5.0       | 1.7 | 2.97    | 0.0031*   |
| <i>Struveopsis</i>   | 4.1       | 1.3 | 3.15    | 0.0017*   |
| <i>Codium</i>        | 2.3       | 0.6 | 4.08    | <.0001**  |
| <i>Padina</i>        | 2.2       | 0.5 | 4.8     | <.0001**  |
| <i>Hydroclathrus</i> | 7.3       | 1.1 | 6.59    | <.0001**  |
| <i>Amphiroa</i>      | 6.8       | 0.8 | 9.05    | <.0001**  |
| <i>Colpomenia</i>    | 5.4       | 0.4 | 14.02   | <.0001*   |
| <i>Spyridia</i>      | -1.5      | 0.7 | -2.10   | 0.0361*   |
| <i>Gracilaria</i>    | -0.9      | 0.4 | -2.18   | 0.0294*   |
| <i>Polysiphonia</i>  | -3.7      | 0.8 | -4.82   | <.0001**  |
| <i>Schizymenia</i>   | -19.1     | 2.1 | -9.33   | <.0001**  |

1259 \*p<0.05, \*\*p<0.001

1260

1261

1262 Table 10. Constant of fitted regression model explaining the  $\delta^{13}\text{C}$  variability by species. Model  
 1263 information includes value of the constant a ( $\delta^{13}\text{C}$ , ‰), standard error (SE), t ratio and Prob > |t|.  
 1264 Only genus with significant effects are enlisted.

| Term                            | $\delta^{13}\text{C}$ , ‰<br>estimated | SE  | Razón t | Prob >  t |
|---------------------------------|--|-----|---------|-----------|
| Model constant                  | -14.6                                  | 0.2 | -93.22  | <.0001**  |
| <i>Hypnea pannosa</i>           | 2.8                                    | 1.3 | 2.24    | 0.0256*   |
| <i>Colpomenia ramosa</i>        | 3.2                                    | 1.4 | 2.27    | 0.0237*   |
| <i>Corallina vancouverensis</i> | 6.3                                    | 2.8 | 2.27    | 0.0238*   |
| <i>Caulerpa peltata</i>         | 3.9                                    | 1.6 | 2.4     | 0.0165*   |
| <i>Codium</i> sp.               | 3.0                                    | 1.3 | 2.4     | 0.0167*   |
| <i>Amphiroa misakiensis</i>     | 7.1                                    | 2.8 | 2.55    | 0.0110*   |
| <i>Jania</i> sp.                | 5.0                                    | 2.0 | 2.56    | 0.0106*   |
| <i>Codium brandegeei</i>        | 2.8                                    | 1.1 | 2.63    | 0.0088**  |
| <i>Hypnea johnstonii</i>        | 3.4                                    | 1.3 | 2.74    | 0.0063**  |
| <i>Tacanoosca uncinata</i>      | 3.4                                    | 1.3 | 2.74    | 0.0062**  |
| <i>Struveopsis</i> sp.          | 4.0                                    | 1.4 | 2.86    | 0.0044**  |
| <i>Padina durvillaei</i>        | 1.4                                    | 0.5 | 2.87    | 0.0043**  |
| <i>Amphiroa</i> sp.3            | 8.2                                    | 2.8 | 2.95    | 0.0033**  |
| <i>Codium simulans</i>          | 3.2                                    | 0.9 | 3.41    | 0.0007**  |
| <i>Amphiroa</i> sp.2            | 6.6                                    | 1.6 | 4.1     | <.0001**  |
| <i>Colpomenia sinuosa</i>       | 4.4                                    | 1.1 | 4.17    | <.0001**  |

|                                   |       |     |       |          |
|-----------------------------------|-------|-----|-------|----------|
| <i>Colpomenia</i> sp.             | 3.6   | 0.9 | 4.27  | <.0001** |
| <i>Padina</i> sp.                 | 3.5   | 0.7 | 4.77  | <.0001** |
| <i>Hydroclathrus clathratus</i>   | 7.2   | 1.1 | 6.82  | <.0001** |
| <i>Amphiroa</i> sp.               | 8.1   | 0.9 | 8.67  | <.0001** |
| <i>Colpomenia tuberculata</i>     | 5.9   | 0.4 | 15.45 | <.0001** |
| <i>Spyrida</i> sp.                | -2.5  | 1.3 | -1.97 | 0.0496*  |
| <i>Pyropia thuretii</i>           | -5.5  | 2.8 | -1.98 | 0.0480*  |
| <i>Ulva acanthophora</i>          | -1.2  | 0.6 | -2.06 | 0.0399*  |
| <i>Grateloupia filicina</i>       | -2.4  | 1.1 | -2.08 | 0.0382*  |
| <i>Rhodymenia</i> sp.             | -4.1  | 2.0 | -2.08 | 0.0380*  |
| <i>Ulva compressa</i>             | -3.2  | 1.4 | -2.33 | 0.0203*  |
| <i>Rhizoclonium riparium</i>      | -5.1  | 1.6 | -3.15 | 0.0017** |
| <i>Polysiphonia</i> sp.           | -4.8  | 1.4 | -3.44 | 0.0006** |
| <i>Halymenia actinophysa</i>      | -9.9  | 2.8 | -3.57 | 0.0004** |
| <i>Cladophora microcladioides</i> | -7.2  | 2.0 | -3.64 | 0.0003** |
| <i>Polysiphonia mollis</i>        | -5.2  | 1.1 | -4.93 | <.0001** |
| <i>Schizymenia pacifica</i>       | -19.2 | 2.0 | -9.76 | <.0001** |

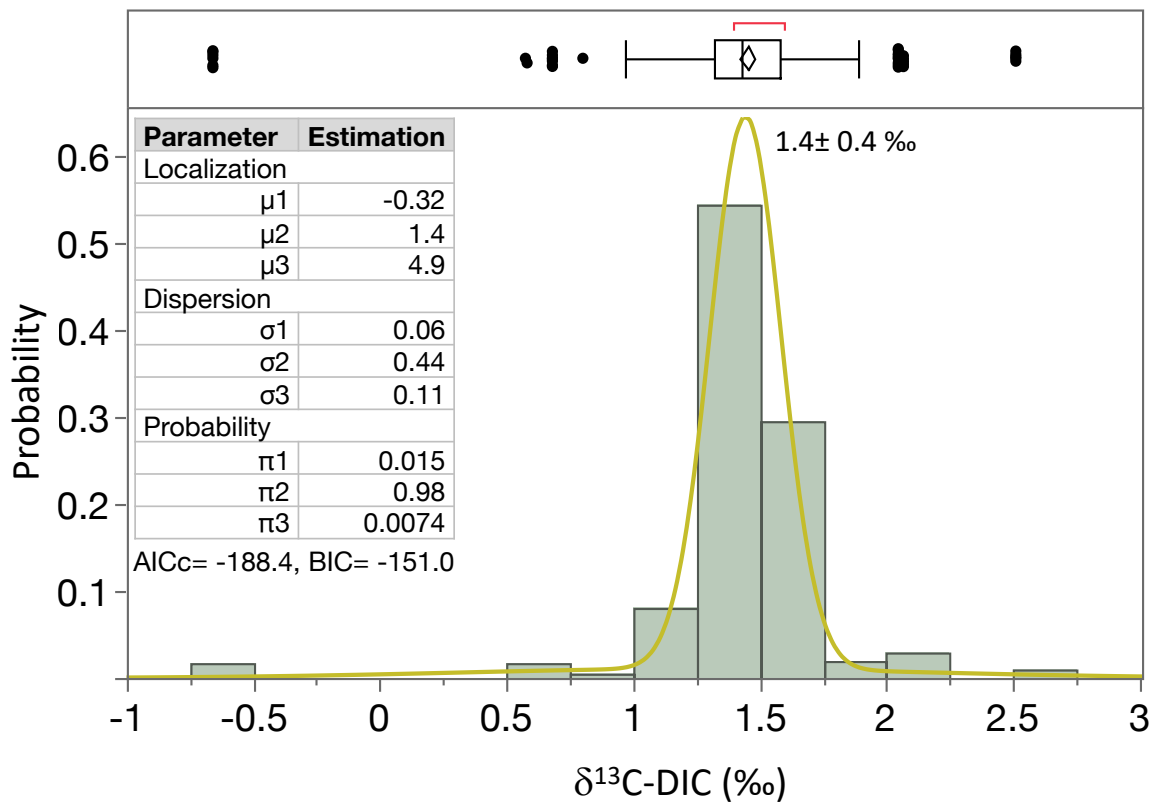
---

\*p<0.05, \*\*p<0.001

1265  
1266



1268

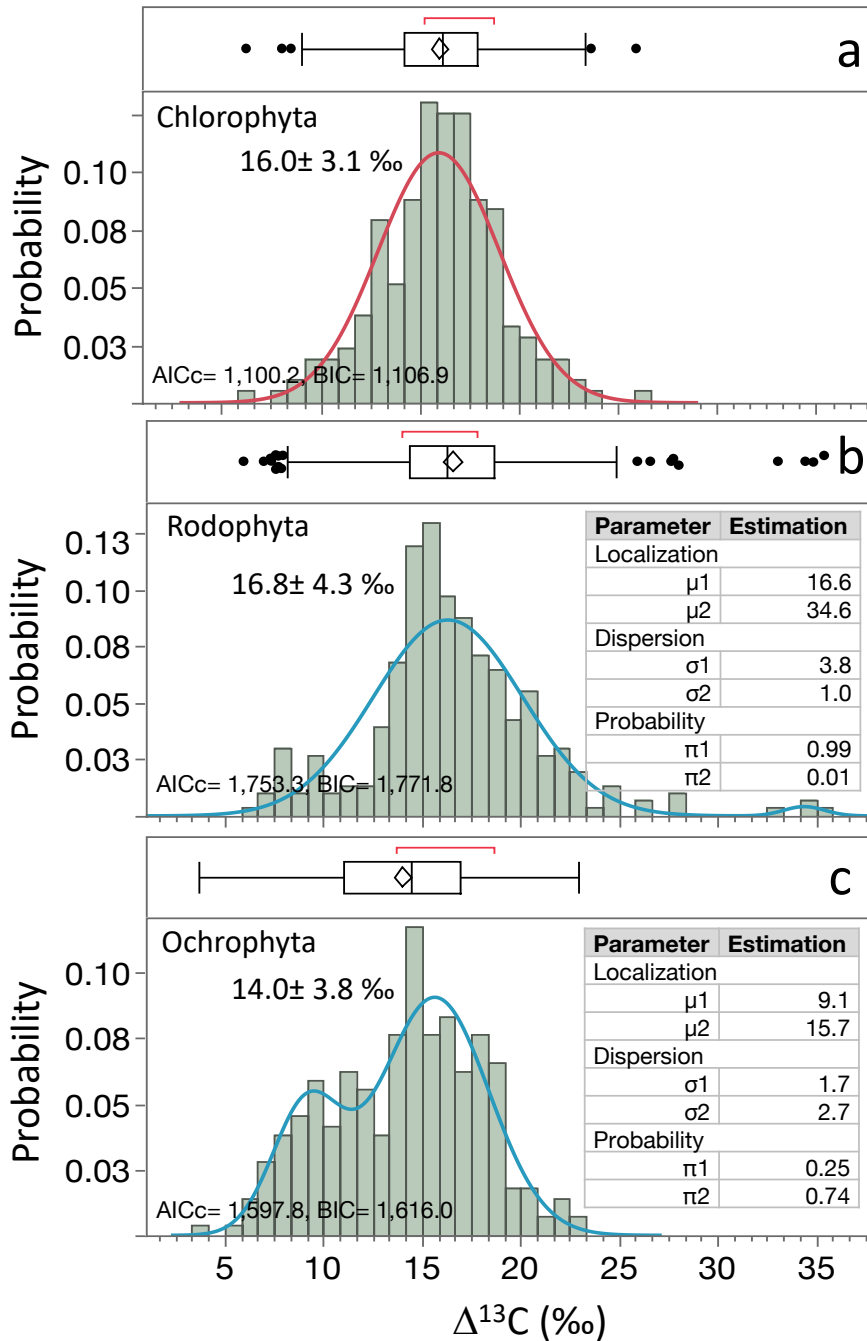


1269

1270 Fig. S1. Histogram representing the distribution of  $\delta^{13}\text{C-DIC}$  values in surface seawater in the Gulf  
 1271 of California.

1272

1273



1274

1275 Fig. S2. Histograms representing the distribution of  $\Delta^{13}\text{C}$ -macroalgal in macroalgae collected in the  
 1276 Gulf of California for Phyla a) Chlorophyta, Rhodophyta, and Ochrophyta.

1277